J Mater Sci (2006) 41:7902–7925
DOI 10.1007/s10853-006-0875-0

Elastic properties of powders during compaction. Part 3: Evaluation of models

M. L. Hentschel · N. W. Page

Received: 16 February 2005 / Accepted: 18 November 2005 / Published online: 13 October 2006

Abstract General approaches for developing models to describe the elastic properties of granular and porous materials are discussed, with emphasis on their application to predicting the elastic properties of powders undergoing uniaxial compaction. Both particle-based, and pore-based models were considered so as to reflect the transition in compact response with decreasing porosity; being particle-dominated at high porosity, then pore-dominated at low porosity. Pore-based models were further subdivided into: mechanistic models, which consider the effects of porosity on internal mechanical fields; and geometric models, for which the elastic response is assumed to correlate with a microstructural feature (e.g. load-bearing area). A selection of models suggested in the literature, considered representative of these approaches, was applied to experimental measurements of the elastic moduli of powders during compaction. In general, the geometric pore-based models show most promise, as these are able to approximate the transition in pore character during compaction. However, further developments are required for application to uniaxially compacted powders. In particular, it is necessary to develop the ability to predict more than one elastic modulus, handle irregular powder particles, and accommodate powders comprised of brittle solid phase materials.

M. L. Hentschel · N. W. Page
Mechanical Engineering, The University of Newcastle, Newcastle, NSW 2308, Australia

Present Address:
N. W. Page (✉)
141 Long St East, Graceville, QLD 4075, Australia
e-mail: npage2@telstra.com

Introduction

Experimental results on the elastic properties of powders during uniaxial compaction have been discussed in companion publications [1, 2], in which a number of results pertinent to the evolution of compact elastic moduli with decreasing porosity were highlighted. Prominent among these is that uniaxial compaction induces significant elastic anisotropy, with the powder compact most generally described as a transversely isotropic material. However, transversely isotropic elastic moduli for the axial plane were found to be qualitatively similar to pseudo-isotropic elastic moduli calculated from axial wave speed measurements and assuming complete isotropy [2]. An extensive suite of such measurements is reported elsewhere [1]; demonstrating the effects of solid phase material properties (yield behaviour, and elastic moduli), and particle shape (pore character) on the porosity dependence of compact elastic moduli.

Attention here is focussed on methods for predicting elastic properties of powders during uniaxial compaction. Important requirements of model behaviour are discussed prior to evaluating a selection of models considered representative of the different approaches suggested in the literature. Included amongst these are models developed for porous materials. As previously discussed [1], the mechanical behaviour of densely compacted powders increasingly approximates that of a porous material as porosity is reduced towards zero. Recognising this transition, it is useful to consider models developed for both granular materials, and porous materials. It is highlighted from the outset that, in many cases, assumptions invoked in model development may not strictly hold for the case of uniaxially

compacted powders; typically models are developed for the respective ends of the porosity spectrum: either pore-based models (low porosity), or particle-based models (high porosity). Despite this, application to powder compaction data is a useful test of model robustness, and provides insight into those features important for development of models specific to compacted powders. Further, many of the observations on model strengths and deficiencies have wider validity than just for the specific case of uniaxial powder compaction data considered here.

Approaches to modelling

Introductory remarks

Relevant models may be divided into two general categories: particle-based models and pore-based models. The particle-based approach considers a medium comprised of discrete solid phase units surrounded by a void matrix, while pore-based models consider a medium formed by placing pores as inclusions into a solid matrix. In general, the particle-based models only cover a small range of porosities starting at a loosely packed state (relatively high porosity). Conversely, pore-based models are confined to the lower end of the porosity spectrum, though they usually encompass a wider range of porosity. In either case, very few models incorporate the deformation of the solid phase material (which is required for significant compaction) in a physically realistic manner. As with experimental work reported in the literature [1, 2], the majority of modelling efforts focus on effective Young's modulus (E), and occasionally bulk (k) or shear (μ) modulus; but only rarely is attention directed towards Poisson's ratio (ν). Quite often only one modulus is considered (usually E). This is an important omission, as at least two elastic moduli are required to completely characterise elastic behaviour (depending on the prevailing isotropy), and hence, models for the porosity dependence of at least two elastic moduli is required.

Aside from the common goals of functional simplicity and accuracy over the entire range of porosity, desirable attributes of models describing the elastic properties of porous and granular materials are given below.

Correct asymptotic behaviour

The model should satisfy the boundary condition of predicting solid phase elastic moduli at zero porosity ($E = E_{\text{solid}}$, and $\nu = \nu_{\text{solid}}$), and also predict the existence of a *critical porosity* (p_c) at which stiffness vanishes: i.e. $E = 0$, and $\nu = 0.5$. For a powder, the critical porosity must fall between the porosities corresponding to the ''tapped'' and ''apparent'' density states, i.e. $p_{\text{tap}} \le p_c \le p_a$ [1, 65]. Hence, in model evaluations discussed later, the value of p_c was constrained to lie within these bounds so as to conserve its physical interpretation.

Consistency with linear elasticity

In addition to requiring the predicted stiffness components to be the inverse of compliances (*self-consistency*), the standard relations of linear elasticity should also hold between all elastic moduli. This can be a useful method of evaluating models. For instance, a common assumption [3, 4] is that normalised shear and Young's moduli follow the same porosity dependence, viz:

$$\frac{E(p)}{E_{\text{solid}}} = \frac{\mu(p)}{\mu_{\text{solid}}}. \tag{1}$$

But, by a well-known relation of isotropic linear elasticity (e.g. [5]):

$$E(p) = 2\mu(p)[\nu(p) + 1]. \tag{2}$$

Equation 1 then implies:

$$\nu(p) = \nu_{\text{solid}}. \tag{3}$$

Thus, if the porosity dependence of normalised shear and Young's modulus were the same, Poisson's ratio would be independent of porosity, remaining constant at its solid phase value. Hence, checking consistency in this manner provides a simple means of validating the relation assumed in Eq. 1.

Physical interpretation

Model parameters should have clear interpretation in terms of a physical property or process. Many models idealise pores (or particles) to a particular geometric shape, commonly spheres or ellipsoids. For a realistic outcome, this should match observed pore (particle) geometry. Further, a direct link should be obvious between the model parameters that describe pore structure and the observed sample microstructure. This is particularly important were the inverse approach to be utilised, i.e. microstructural characterisation by measurement of elastic properties.

In addition to these quite general requirements for modelling physical properties of both porous and granular materials, it is also felt that the distributed nature of interactions between particles (or pores) should be incorporated in model development. Usually, the behaviour of a representative sub-system of the medium (e.g. a single particle–particle interaction, or a single pore in an infinite matrix) can be accurately described; certainly for simple boundary conditions (e.g. contacting spheres, or an isolated ellipsoidal inclusion). However, granular and porous materials of practical interest typically comprise a very large number of such sub-systems. Two difficulties then arise when attempting to extrapolate sub-system behaviour to a corresponding bulk property. First, each sub-system is generally not identical, e.g. particles may contact at different angles, pores may have different shapes, etc. Thus, considering a single ''typical'' sub-system may not suffice. Second, due to differences between each sub-system, and interaction between sub-systems, it is unlikely that each is subject to the same mechanical fields (stress or strain), and thus, significant variation in response may be expected. However, uniform and closely reproducible physical properties are observed in macroscale behaviour. Thus, it is suggested that prediction of elastic behaviour (and other physical properties) requires first an understanding of the basic interactions, and second, application of an appropriate averaging (homogenisation) procedure for transferral of these interactions to the bulk. This second point appears the most challenging, with a variety of approaches suggested in the literature. Model development often commences by considering a medium idealised as either a particle assemblage, or a solid matrix material with inclusions of a specific type of porosity. Discussion in the following centres on salient features of such particle-based and pore-based approaches to modelling; specific examples are considered later (see ''Evaluation of specific models''), including a comparison with experimental data.

Particle-based models

Many particle-based models idealise the granular assemblage as a regular packing of identical spheres (simple cubic, face-centred cubic, etc.). In such models (e.g. [6–11]), particles are represented by spheres to simplify the particle–particle interactions. The assumption of a regular packing provides homogenisation, with the properties of a small group of contacting spheres (a representative sub-system) taken to be equivalent to that of the bulk. Note that only those models in which the particles retain their individual identity are discussed here: other models (e.g. [12, 4]) which consider particle packings, but with continuous solid phase bonding at inter-particle contacts are discussed later (see ''Mechanistic pore-based models (Transversely isotropic)'').

To idealise a granular material as a regular packing of spheres is conceptually simple; however, there are a number of concerns. First is the ability of spheres to accurately replicate particles of a real granular material. Powder particles often deviate significantly from identical spheres (or other simple geometric shapes). Hence, the assumption of regularly stacked monosize particles is unlikely to be realised in practice: a different sized, or non-spherical particle will perturb the assumed packing [12], and thereby alter the uniformity of physical properties (e.g. [13, 14, 6]). Further to this, regular packings have inherent anisotropy [12] with elastic stiffness changing according to the direction and nature of applied stress. Many models based on regular sphere packings are solved only for a particular loading condition, most often uniaxial loading along $<1\ 0\ 0>$ (e.g. [4]). By analogy with crystalline materials, it may be possible to consider the bulk granular material as comprised of randomly oriented domains (grains) of regular packings, with the isotropic response approximated by averaging over many different lattice directions. However, unlike atoms, it is not energetically favourable for powder particles to assume regular positions, and as such, domain sizes will be quite small with a large fraction of particles at domain boundaries. As a result directional averaging alone is unlikely to suffice. To better approximate real granular materials, several researchers have considered random packing of both spherical particles (e.g. [15–20]), and non-spherical (typically ellipsoidal) particles (e.g. [21, 22]). Some also consider different sized particles (e.g. [15, 23–26]). However, these models still suffer the significant disadvantage of being unable to handle changes in compact microstructure which result from permanent solid phase deformation of particles as porosity is reduced during compaction. Most particle-based models only consider elastic deformation about a particular packing arrangement (random or regular). This essentially limits their validity to a single value of porosity (or at best, for porosity changes due solely to particle rearrangement). Thus, although porosity may appear as a model parameter, it simply defines the packing state for which the elastic properties are solved. Similarly, applied stress often appears as a model parameter; again though, it is generally assumed to cause elastic deformation only, not the permanent solid phase deformation of particles inevitable during large-scale powder compaction.

An example of this approach to modelling is furnished by the model for the effective Young's modulus of packings of identical spheres developed by Kendall et al. [8]. Assuming the relation between inter-particle contact area and applied load conforms to ''JKR'' contact mechanics, an equation for Young's modulus of a simple cubic sphere packing was obtained, viz:

$$E = \left[\frac{9\pi\Gamma E_{\text{solid}}^2}{16D(1-\nu_{\text{solid}}^2)^2}\right]^{1/3} \quad (4)$$

where Γ: interface energy (energy to separate a unit area of plane surfaces), D: particle diameter.

For other regular packings of identical spheres (hexagonal close-packing, etc.), expressions similar to Eq. 4 were obtained [8]. Kendall and co-workers found that, if predicted Young's modulus was plotted against porosity for each packing, the points fell close to a simple curve given by Eq. 5 (see subsection ''Kendall et al. (1987)''). However, in the development of this model equation, the porosity changes considered were due solely to particle rearrangement: permanent deformation of the particle material (plastic flow of particle material, particle fracture, etc.) was not considered. As such, Eq. 5 represents a locus of possible Young's modulus depending on efficiency of packing, with particles retaining their initial shape (spherical) at each level of porosity. Consideration of Eq. 5 at $p = 0$, demonstrates that, in general, the required boundary condition of $E = E_{\text{solid}}$ is not satisfied (see subsection ''Kendall et al. (1987)''), suggesting poor predictive performance as compact density increases towards solid. This is not particularly surprising, as the assumed regular packings of perfect spheres will certainly not be valid in this porosity region; particles of a real granular material would be heavily deformed, bearing little resemblance to spheres.

Pore-based models

Introductory remarks

Many equations have been suggested to describe the elastic properties of porous materials. The majority of modelling is approached by considering effects of adding discrete pores to a solid phase matrix (instead of discrete particles to a void matrix). In order to make the attendant mathematics tractable, many idealisations of a real porous material, and assumptions of its behaviour are required. Common assumptions are spherical, isolated, non-interacting pores (e.g. [27–30]). The primary advantage of a spherical pore is the simplicity of surrounding mechanical fields. However, in many materials of practical interest, spheres are unlikely to accurately replicate the true porosity, particularly at high porosities where extensive pore interconnection is expected. Attempts to more accurately describe realistic porosity have been made by assuming the pores can be represented by ellipsoids, varying from prolate to oblate (e.g. [31–36]), often utilising results due to Eshelby [37] on the effect of an isolated ellipsoidal inclusion in a homogeneous matrix. Pore shapes other than ellipsoidal will have complex stress concentrations, but have been considered (e.g. [38–40, 36]). In each, the pore is still assumed to be a single, definable feature (closed porosity): interconnection and unbounded pore space are not explicitly considered.

Models for the elastic properties of porous materials may be broadly classified according to the basic approach used [12]. The first type of model approach, denoted as *mechanistic*, considers the effect on mechanical fields when porosity is included into a solid phase matrix. Often this is achieved as a limiting condition of a two-phase composite material, with properties of the inclusion phase set to empty space (void). Typically, elastic moduli are evaluated by considering effects of adding an inclusion (pore) to a representative volume element (sub-system) of the material. The average strain in this element is related to the average stress (or the converse), and the effective properties are then transferred to the macroscale by use of a suitable homogenisation (averaging) scheme. Other approaches based on wave scattering have also been used (e.g. [30]). The second general approach to modelling elastic properties of porous materials are *geometrically* based [12]. In such models, a certain geometric feature of the microstructure is assumed to be directly linked to the elastic behaviour. Such models are typically less rigorous, as the link may not be physically based; however, this approach has the strong advantage of being able to handle a wide range of porosities [12].

Mechanistic pore-based models

Perhaps the simplest models for achieving property averaging consider either the stress throughout the entire material to be uniform (Reuss model), or assuming uniform strain throughout (Voigt model) [41]. Predictions of the two approaches are often averaged, or used in tandem to provide bounds for elastic moduli of a composite material. Provided the elastic moduli of matrix and inclusion phase do not differ by much more than a factor of two, such bounds

are reasonably narrow [41]. However, for the extreme case of a porous material, they are too wide to have useful application. Narrower bounds for elastic moduli of composite materials have also been derived (e.g. [28, 42, 43]). However, when following this approach, care should be taken to ensure a realistic microstructure is obtained when the properties of one phase are set to those of empty space (void). Some other homogenisation schemes which have been used to obtain estimates of elastic moduli of porous materials are discussed briefly in the following; more extensive descriptions are available elsewhere [36, 44–48].

(i) *Non-interacting inclusions (dilute concentration)*. This method considers a single inclusion added to an infinite matrix of solid phase material which is subject to uniform far-field stress (or strain). Commonly, the inclusion is idealised to a regular shape; often using the results of Eshelby [37] for an ellipsoidal inclusion in an infinite matrix. Inclusions are assumed to be separated by a sufficiently large distance so that interactions can be neglected. That is, the perturbation to mechanical fields (stress and strain) caused by one inclusion does not affect the uniformity or magnitude of the field around adjacent inclusions. In practice, inclusion (pore) placement will be approximately random; thus the requirement for non-interacting inclusions will generally hold best for low inclusion concentrations (low porosity). Rice [12] suggests pore interaction becomes significant when adjacent pore surfaces are separated by a distance approximately equal to their size. For equal spherical pores, stacked in a simple cubic array (often considered indicative of random packing), this would restrict applicability to porosities less than approximately 0.2. Random placement of pores is expected to produce a number of instances where the minimum distance between pores is quite small [36]; and thus, in practice, the non-interacting pore assumption is likely to hold only at the lowest porosity levels ($p < 0.1$ [49]). For application to powder compaction, significantly higher porosities need to be considered; hence the non-interacting inclusion approach itself is not considered in detail here. However, results for the non-interacting case often form the basis of other homogenisation schemes that do incorporate effects of interaction, discussed in the following. Finally, it is noted that interaction between pores may be beneficial for reducing stress concentrations and to assist in uniform transfer of stress throughout the medium [12].

(ii) *Self-consistent scheme*. The basis of the self-consistent scheme is again consideration of an isolated inclusion placed into a homogeneous effective matrix. However, in contrast to the case of non-interacting inclusions, matrix properties are not taken to be those of the solid phase material: the assumed elastic properties of the (effective) matrix are those of the bulk material [34]. This approach thus accounts for pore interaction by acknowledging the effect nearby porosity has on modifying the matrix properties from those of the solid phase material. The disadvantage of this scheme is that models for porous materials generally predict vanishing elastic properties at $p = 0.5$ due to an implicit assumption of symmetry between inclusion and matrix phases [50, 51, 46]. This feature is clearly undesirable, as many granular and porous materials have measurable elastic properties for porosities greater than 0.5. Further, practical implementation is hampered by the cumbersome nature of the equations, which in addition to being mathematically complex, require iterative solution techniques (see, for example [51, 34]).

(iii) *Differential method*. This method initially considers a solid matrix containing an infinitesimal amount of inclusions, with effective properties calculated by the non-interacting inclusion method. As the number of inclusions is small, the non-interacting method will be valid. The solid matrix is then replaced by a homogeneous matrix with the properties just calculated, to which another infinitesimal amount of inclusions are subsequently added. Again, the non-interacting inclusion method is invoked to find the effective properties of this new material. In turn, these properties are assigned to a new homogeneous matrix, to which another infinitesimal amount of inclusions are added. This procedure is repeated until the desired inclusion concentration level is obtained [44]. Zimmerman [29] has derived a model for the elastic moduli of a composite with spherical inclusions using this method. However, by consideration of the effects of adding cracks to the material, Kachanov et al. [36] argue that both this method and the self-consistent scheme are insensitive to the average stress in the matrix, a situation they suggest is physically unreasonable.

(iv) *Mori–Tanaka method*. The Mori–Tanaka method [52] differs from (ii) and (iii) above, in that the bulk properties are obtained by considering an inclusion subject to an effective field (stress or strain), rather than being placed in an effective matrix. Dvorak and Srinivas [53] and, Nemat-Nasser and Hori [44] discuss the similarities between this approach and those described above in detail. Models applicable to porous materials have been derived using the Mori–Tanaka method by, for example: [35, 36, 54, 46, 55]. Kachanov et al. [36] argues that the Mori–Tanaka approach is superior to the self-consistent and

differential methods of homogenisation. Ferrari and Filipponi [56] also found the Mori–Tanaka method provided a better fit to data on porous ceramics than the self-consistent scheme or non-interacting inclusion method. However, Ponte Castañeda and Willis, [57] caution that the Mori–Tanaka method is not always appropriate, citing examples involving anisotropic distribution of inclusions, and mixes of inclusion shapes and orientations.

(v) *Composite sphere model*. The composite-sphere model originally considers the porous body to be constructed of composite spherical particles consisting of a spherical shell of matrix material surrounding a concentric spherical inclusion [28]. The ratio of the phases in each composite sphere is equal to the overall ratio of matrix to inclusion phase of the body. It is assumed the composite spheres are available in an infinite range of sizes, so that all space can be filled by inserting suitably sized spheres in the interstices between packings of other (larger) spheres. Stress applied to the body is assumed to be uniformly distributed (hydrostatic) around the inclusion in each composite sphere so that strains can be calculated to obtain elastic moduli for the body [47, 48]. Various extensions to the basic composite-sphere model have been made (e.g. [32, 39, 40, 45]). An obvious disadvantage of this modelling approach is the required size distribution so that all interstitial space is completely filled. Further, all inclusions (pores) are assumed to be isolated by matrix material. Neither assumption is likely to be met in practice.

Geometric pore-based models

Typical of the geometric models is the load-bearing area concept discussed in a series of publications by Rice [47, 48, 58, 12], and also by Cytermann [59]. In these models, normalised Young's modulus of the porous material is assumed to equal the normalised load bearing area (the area of solid phase material per unit area in a cross-section perpendicular to the direction of stress application). Most of the discussion by Rice is based around porous materials with idealised microstructures, constructed from regular packings of either pores in a solid matrix, or solid spheres in a void matrix (empty space). With such microstructures, a number of possible load-bearing areas exist, depending where the cross-section is taken through the packing. Rice [12] argues minimum solid area (MSA) is most appropriate of the various load-bearing areas (average, maximum, minimum, etc.). MSA is the smallest cross-sectional area of solid phase material in the plane perpendicular to the direction of stress application. MSA normalised by unit area (NMSA) is then assumed [12] to equal to the effective property of interest, i.e. $E/E_{\text{solid}} = \text{NMSA}_{\perp}$. Throughout the following "$\text{NMSA}_{\perp}$" denotes normalised minimum solid area of the plane perpendicular to the loading direction, while "$\text{NMSA}_{||}$" is the normalised minimum solid area of the plane parallel to the direction of loading. In the MSA modelling approach, effects of pore character are incorporated implicitly within the model, and do not appear as a quantitative model parameter. This approach has several attractive features:

- Both pore-based and particle-based materials and handled in the same manner.
- The transition from interconnected to isolated pore structures is incorporated.
- Boundary conditions are satisfied. At $p = 0$; $\text{NMSA}_{\perp} = E/E_{\text{solid}} = 1$. Alternatively, at $p = p_c$; $\text{NMSA}_{\perp} = E/E_{\text{solid}} = 0$.
- Densification by permanent solid phase deformation is included in a realistic manner (particularly for ductile materials).

The final point is particularly advantageous as it incorporates changes in microstructure with porosity. However, there are also a number of disadvantages to this approach. Particular among these is that more than one elastic modulus is required for complete elastic characterisation (i.e. solution of Hooke's law for a general triaxial stress state). Two elastic moduli are required (commonly E and ν are used) to describe a medium which is elastically isotropic; if the medium is elastically anisotropic, more moduli are required. This appears to be neglected in the discussion of MSA models, which provide a description of E/E_{solid} only. Presumably, if an analogous model were to be developed for a second elastic modulus, MSA would still the most appropriate of the possible load-bearing areas. However, while the choice of $\text{NMSA}_{\perp}$ for normalised Young's modulus is reasonable, if not completely rigorous, a similar choice of MSA for other moduli is not obvious. For Poisson's ratio, no single MSA seems appropriate. If the analogy held with Poisson's ratio defined in terms of material strains, the ratio of $\text{NMSA}_{||}$ to $\text{NMSA}_{\perp}$ would be appropriate. However, were this to be the case, then $\nu(p) = \text{NMSA}_{||}/\text{NMSA}_{\perp} = 1$ for model microstructures formed by regular packings of pores or particles. Similarly, for shear modulus, $\mu/\mu_{\text{solid}} = \text{NMSA}_{\perp}$ seems the most likely candidate. But, for a regular packing, $\text{NMSA}_{\perp} = \text{NMSA}_{||}$, and thus, $\mu/\mu_{\text{solid}} = E/E_{\text{solid}}$ which, by Eqs. 1–3, implies Poisson's ratio is constant at the

solid phase value for all porosities. Neither situation matches observed behaviour. It is noted however, that this very behaviour will often make a given MSA model for Young's modulus less susceptible to issues of anisotropy. For instance, in the MSA model based on simple cubic sphere stacking MSA is the same in <100>, <110> and <111> [12, 48].

The other main disadvantages of the MSA approach are common to those of all models considered thus far. These are: first, the ability to accurately reflect the physics of the true microstructure, and second, interpretation of model predictions. Most MSA models are generated considering a single type of porosity (this gives each its particular porosity dependence). However, in practice, it is inevitable that the nature of the pore character will evolve with porosity changes. For example, in the initial stages of sintering a compact of mono-sized spherical particles, one of the MSA models for identical spherical particles would be applicable. However, as the bulk density approaches that of the solid phase, the pores will become increasingly spherical (due to preferential growth of necks at interparticle contacts). In this stage, a MSA model for a regular packing of spherical pores would be most appropriate. Transition from one model to another can be accounted for by interpolation using a porosity dependent weighting for the different model components [12]. However, the MSA-porosity curve resulting from such a scheme would no longer be unique to a porosity type: the same values could be generated by a combination of other porosity types. Thus, while MSA models do consider some evolution of sample microstructure, further issues remain to be resolved. Still, it is felt that the microstructural changes contained within a single MSA model still provides a more realistic description of compaction-induced porosity changes than the mechanistic models discussed previously.

A further issue for practical utilisation of MSA models is measurement of NMSA in real material microstructures. For the periodic microstructures that result from regular packings of particles or pores, the definition of MSA is straightforward: the smallest contact areas lie on a single well-defined plane (Fig. 1a). Further, MSA is unique for such a microstructure. However, for the more realistic microstructure of Fig. 1b, the definition of MSA is less clear. In this case the smallest areas of contact do not lie on a single plane, but are distributed throughout a finite sample thickness. A further practical consideration is the undoubted spatial variation in MSA in a real material. In a periodic structure, the global MSA will be equal to the local MSA (taken on the length scale of particle size). However, in a real material this will not be the case: in addition to a global minimum, several local minima would be expected. While a global MSA is simply defined, utilising this value would suggest all deformation is confined to a specific area of the sample. An alternative, such as taking the average of local MSAs, would require averaging of local minimum properties. This would be difficult to perform in a truly objective manner; though in practice, it is likely that a reasonable ''working'' definition could be formulated, particularly if supported by experimental measurements of MSA (e.g. from specimen tomography, or a suite of cross-sectioned samples).

Evaluation of specific models

Introductory remarks

A large number of models have been suggested in the literature. In the following, a selection of models, considered representative of the approaches described in ''Approaches to modelling'' are discussed further and compared with results of uniaxial powder compaction experiments described in a previous work by the authors [1]. As exclusively empirical models reveal little of the physical processes that underpin elastic behaviour, they are not considered here (see [3, 60] for a discussion of such models). When selecting specific models to evaluate, three main features were considered: (i) physical interpretation of model parameters, (ii) whether a complete description of elastic behaviour is provided, and (iii) ability of the model to satisfy boundary conditions.

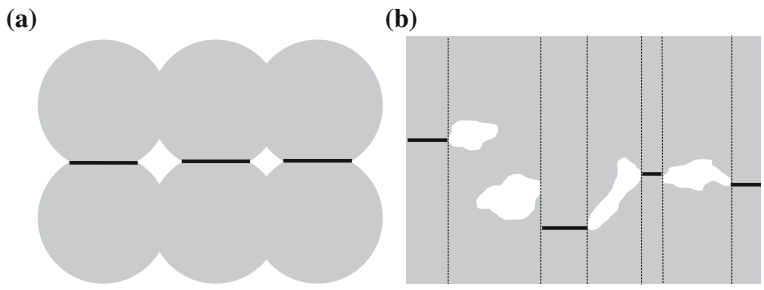

Fig. 1 Definition of minimum solid area (MSA). MSA is shown by the bold lines. (**a**) Model based on a simple cubic packing of identical spheres. MSA is the cross-sectional area at particle contacts. (**b**) A more realistic sample microstructure. In this case, the MSA does not lie on a single plane

Due to their inability to handle the large changes in porosity associated with significant compaction, only one particle-based model is considered here, that due to Kendall et al. [8]. This model is considered broadly representative of those based on particle packing that admit elastic deformation only. Because of this limitation, such models are only applicable at the highest porosities considered in this study. At lower porosities, the assumed contact geometry will be invalidated by permanent deformation of the particle material induced by compaction. Models derived for porous materials are generally more robust to changes in porosity; thus, a number are considered, drawing from those representative of mechanistic and geometric approaches. As the experimental data considered extends to high porosities, no dilute–concentration mechanistic models are considered. Of the remaining homogenisation techniques, the approach of Nielsen [40] (composite sphere method), and Zhao et al. [35] (Mori–Tanaka method) are considered. Of the geometric models for porous materials, the minimum solid area models of Rice [12] are discussed, along with the model of Wang [4]. Both models are based on load-bearing area, though each considers a slightly different distribution of deformation throughout the material. Although models that predict both E and ν are preferred, the equation of Boccaccini et al. [61] is also included as it is used subsequently used in the model of Arnold et al. [62] for prediction of $\nu(p)$. This latter model is of interest as it displays the ability to qualitatively replicate the concave porosity dependence of ν evident in the experimental data [1].

Particle-based models

Kendall et al. (1987)

This model is based on a calculation for effective Young's modulus of a variety of different spherical particle packings (see section ''Approaches to modelling'' under subsection ''Particle-based models'')

$$E = 17.1\left(\frac{E_{\text{solid}}^2\Gamma}{D}\right)^{1/3}(1-p)^4. \tag{5}$$

Model parameters: $E = E(E_{\text{solid}}, \Gamma, D, p)$. Γ is the interface energy (energy required to separate a unit area of plane surfaces). D is particle diameter.

Boundary conditions: As discussed in ''Approaches to Modelling'' subsection ''Introductory remarks'', two boundary conditions are of interest. At $p = 0$, the predicted elastic moduli should coincide with solid phase values; and a critical porosity (percolation threshold), p_c should be predicted at which material stiffness vanishes. For a granular material p_c is expected to lie within the range of gravity-induced packing states $p_{\text{tap}} < p_c < p_a$ [1], where p_{tap} and p_a are porosities of the ''tapped'' and ''as-poured'' packing states, respectively. For powders, p_c is less than unity, e.g. for spheroidal copper it has been found that $0.370 < p_c < 0.423$ [1].

For the model of Kendal et al. when $p = 0$: $E = 17.1\left(\frac{E_{\text{solid}}^2\Gamma}{D}\right)^{1/3}$. At $E = 0$: $p = p_c = 1$, for finite Γ.

Thus, model predictions at these two limiting values suggest this model is not applicable to powder compaction. The required boundary condition of $E = E_{\text{solid}}$ at $p = 0$, will only be satisfied for a particular value of particle size (D), assuming Γ is constant for a given material (interface). For the example of glass powder, this condition is satisfied only for $D = 3.1$ nm, using $\Gamma = 0.04$ J m^{-2} [63] and $E_{\text{solid}} = 64$ GPa. Such a situation is unrealistic, though not surprising, given this model assumes particles retain their spherical shape throughout.

The lower boundary condition of the model, which predicts $E = 0$ only at $p = 1$ is also physically unrealistic. This arises from the use of an empirical equation (5) to approximate the porosity dependence of effective Young's modulus calculated for a variety of particle packings (such as Eq. 4 for a simple cubic packing). The inability to accommodate critical porosities less than unity is a common failing of many models discussed in the following, and is one of the main contributors to poor predictive ability of this and several other models considered here. Predictions for the model of Kendall and co-workers over a wider porosity range are presented in the following.

Model predictions: Figure 2 presents a comparison of the Kendall et al. model predictions, and experimental data for three different powders. For clarity, experimental data is restricted to a sub-set of the different powders discussed elsewhere [1]. The three selected (spheroidal glass, spheroidal copper, and dendritic copper powders), are considered representative: spheroidal copper and spheroidal glass powders illustrate the influence of solid phase yield mechanism, while the dendritic and spheroidal copper powders demonstrate particle shape effects. To test predictions of Eq. 5, Γ was used as a fitting parameter; D was fixed at 90.5 μm, as all powders had been sieved to select the +75–106 μm size fraction. Generally, a reasonable fit results; however, fitted values of Γ are far in excess of expected values. For the glass powder compact, the fitted value $\Gamma = 120$ J m^{-2}, is some three orders of

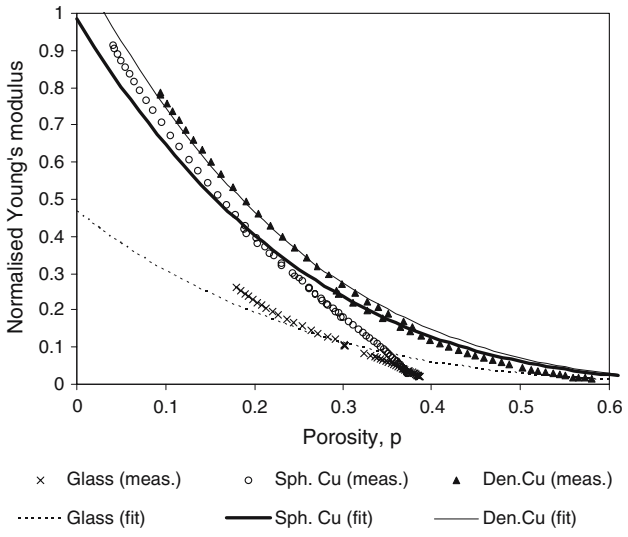

Fig. 2 Predictions of the model of Kendall et al. (Eq. 5) compared to experimental data from [1]. Γ was used as a fitting parameter; see also Table 1. Spheroidal glass: (×) measured, (- - - -) fitted. Spheroidal copper: (○) measured, (—) fitted. Dendritic copper: (▲) measured, (–) fitted

magnitude higher than literature values (0.04 J m^{-2}) [63]. Also for copper: Γ is 1.96 J m^{-2} [64] whereas the fitted values were 1,990 and 3,050 J m^{-2}, for spheroidal and dendritic copper powders, respectively. Given that Γ represents the strength of adhesion between otherwise free surfaces, an increase in Γ is consistent with enhanced inter-particle bonding as compaction proceeds. However, in the present case, stronger bonding is not solely due to surface forces; the dendritic powder in particular will have a component due to particle interlocking that results from plastic flow of the solid phase material. Extension of Γ to a more general parameter representing inter-particle bond strength (i.e. one which incorporates both surface adhesion, and interlocking effects) is of doubtful value, as this is not consistent with the basic interaction considered in the model (i.e. particle bonding due to surface forces only). Further, the contribution of particle interlocking will change during compaction. Thus a single value of such a redefined Γ would not be appropriate to describe the porosity evolution of elastic moduli (a point discussed in more detail in subsection ''Boccaccini et al. (1993)''). Of perhaps greater importance though, is that the assumed microstructure of the model (identical spherical particles) was rarely approached experimentally (micrographs of highly deformed particles recovered from powder compacts are presented elsewhere [65]). This deviation from assumed microstructure will also affect model predictions. For the spheroidal particles in particular, the model of Kendall et al. (Fig. 2) underestimates Young's modulus at low porosity, and overestimates at high porosity; an unsurprising result since the model admits only elastic deformation between touching spheres. As deformation proceeds by compaction, the area of solid phase contact must grow (on average), and hence the stiffness will rise, as observed.

Mechanistic pore-based models (Isotropic)

Nielsen (1982)

The model of Nielsen [40] is included as an example of models for porous materials based on the composite sphere approach to homogenisation (see section ''Approaches to modelling'' under subsection ''Mechanistic pore-based models''). The resulting equations for Young's modulus and Poisson's ratio are:

$$E = \frac{2\beta E_{\text{solid}}(1-p)(5\nu_{\text{solid}}-7)(p_c-p)}{2\beta(5\nu_{\text{solid}}-7)(p_c-p)+p_c p(\nu_{\text{solid}}+1)(15\nu_{\text{solid}}-13)} \quad (6)$$

$$\nu = \frac{2\beta\nu_{\text{solid}}(5\nu_{\text{solid}}-7)(p_c-p)+p_c p(\nu_{\text{solid}}+1)(5\nu_{\text{solid}}-3)}{2\beta(5\nu_{\text{solid}}-7)(p_c-p)+p_c p(\nu_{\text{solid}}+1)(15\nu_{\text{solid}}-13)}. \quad (7)$$

Model parameters: $E = E(E_{\text{solid}}, \nu_{\text{solid}}, p, p_c, \beta)$, and $\nu = \nu(\nu_{\text{solid}}, p, p_c, \beta)$. β is a shape factor which characterises transfer of stress within the solid matrix, incorporating information on both the shape of pores and their interconnection ($0 < \beta < 1$). Nielsen [39, 40] suggests β can be interpreted as representing the tendency for one phase to ''cleave'' the other into discrete units. The lower limit is $\beta = 0$, when the pore phase totally surrounds solid phase particles. Due to the phase symmetric nature of the model, the alternative is also possible; $\beta = 1$ represents the upper bound, when solid phase material totally surrounds the pore phase, i.e. isolated pores. Thus, low values of β correspond to strongly interconnected pores (small solid phase contact area), while higher values indicate the pores are becoming increasingly isolated. There is also an effect due to pore character; with isolated, non-spherical pores found to produce $\beta < 1$ [39]. However, beyond this, the relationship of β to the sample microstructure, and in particular the microstructural features that would need to be measured for prediction of β, is not clear. Equations 6, 7 show a functional dependency of elastic moduli with porosity and β such that a smaller value of β causes a more rapid decrease of each elastic modulus with porosity (for fixed ν_{solid}

and p_c). Further details are provided in [65]. To further assist interpretation of β, in [65] the equations of Nielsen were applied to the data of Roberts and Garboczi [49] from finite element modelling of idealised microstructures. This provided indicative β values of 0.92 for a microstructure based on spherical pores; 0.49 for ellipsoidal pores; and 0.37 for a microstructure formed from bonded solid spheres [65]. Equations 6, 7 both depend on Poisson's ratio of the solid phase material. For fixed β and p_c, the effect of ν_{solid} on Young's modulus (Eq. 6) is negligible. In contrast, ν_{solid} strongly affects the nature of the evolution of ν with porosity in this model. For $\nu_{solid} > 0.2$, ν decreases with porosity, whereas $\nu_{solid} < 0.2$ produces an increase of ν with p, and ν is independent of porosity at $\nu_{solid} = 0.2$ [65].

Boundary conditions: When $p = 0$: $E = E_{solid}$, $\nu = \nu_{solid}$. At $E = 0$: $p = p_c$, and $\nu_c = \frac{5\nu_{solid}-3}{15\nu_{solid}-13}$. These two conditions also result for $\beta = 0$. Given that $-1 \le \nu_{solid} \le 0.5$ for an isotropic material, the critical value of Poisson's ratio must lie within the range $0.09 \le \nu_c \le 0.29$. Further, for many materials (certainly all studied in this work), $\nu_{solid} > 0$, and hence $0.09 \le \nu_c \le 0.23$.

The Nielsen model satisfies the boundary conditions quite well, correctly predicting both solid phase elastic moduli at zero porosity, and the existence of a critical porosity (p_c) for which $E = 0$. However, the prediction of $0.09 \le \nu_c \le 0.23$ is significantly lower than the value of 0.5 predicted on the basis of physical reasoning that air is the stress transmitting medium at the point where the solid phase ceases to support load [1]. As seen in the following, this has important implications on the quality of model predictions for ν.

Application of Nielsen's model to experimental data is illustrated in Fig. 3. For consistency between elastic moduli, both sets of data were regressed simultaneously, by minimisation of the objective function defined by Eq. 8 (following Martin et al. [46]). Regression parameters for the model of Nielsen are provided in Table 1.

$$\sum_{i=1}^{n}\left[\left(\frac{E_{experimental}-E_{predicted}}{E_{experimental}}\right)^2+\left(\frac{\nu_{experimental}-\nu_{predicted}}{\nu_{experimental}}\right)^2\right] \quad (8)$$

for a (p, E, ν) data set of n points.

As discussed above, and elsewhere [1], for a powder, p_c is expected to lie within the range $p_{tap} \le p_c \le p_a$, thus in the regression, p_c was only allowed to vary within this range. For the model of Nielsen, p_c converged to a stable value within this range for all powders except the dendritic copper powder which was constrained by the minimum value (p_{tap}), see Table 1. Removal of this constraint provided a better fit, but at the expense of a clear physical interpretation for p_c. No constraints were placed on the shape factor β.

The predictive ability of Eq. 6 compares reasonably with the experimentally measured Young's modulus, particularly for those powders that p_c converged to a value in the range $p_{tap} < p_c < p_a$. However, Fig. 3b indicates poor agreement of the model with the data of Poisson's ratio, particularly at high porosities. This was consistent among all powders [65], and seems to be due to the lower boundary condition of $0.09 \le \nu_c \le 0.23$. The requirement for the model equation to satisfy this boundary condition means the observed rise in ν at high porosities is unable to be replicated by the model of Nielsen.

The general agreement between fitted values of p_c and those expected from packing tests (Table 1) [1, 64] is encouraging, and illustrates the benefits of accounting for vanishing material stiffness at porosities less than unity. When the model did not accurately predict p_c, its predictive ability for Young's modulus diminished noticeably (e.g. dendritic copper powder). Fitted values of the shape factor, β generally correlated with expected trends. However, the ability of β to discriminate between different microstructures was not always successful. While able to differentiate between ductile and brittle spheroidal powders, particle shape differences within the ductile powders did not produce a strong effect on β. Table 1 indicates β for spheroidal metal powders spans a range of 0.027, whereas the β value of the irregular copper (US) powder is only 0.026 lower than for spheroidal aluminium. Similarly, the range of β values within the group of irregular metal powders is substantial (0.084). Thus, the ability to identify a microstructure purely on the basis of the best-fitting β value is questionable. A more basic problem with the values of β obtained from this model, is that the microstructure is described by a single parameter. From sectioned compacts of irregular copper powder (US Bronze) [65], the porosity was found to be largely closed and approximately isometric at low porosities ($p = 0.08$); while at higher porosities ($p = 0.31$), porosity was much more open and interconnected. Using Nielsen's suggested interpretation of β as described above, β should be close to unity (isolated spherical pores) at porosities close to zero. Conversely, β should approach zero at high porosities. Thus, for significant compaction of a powder, a single value of β is not appropriate: compaction induces

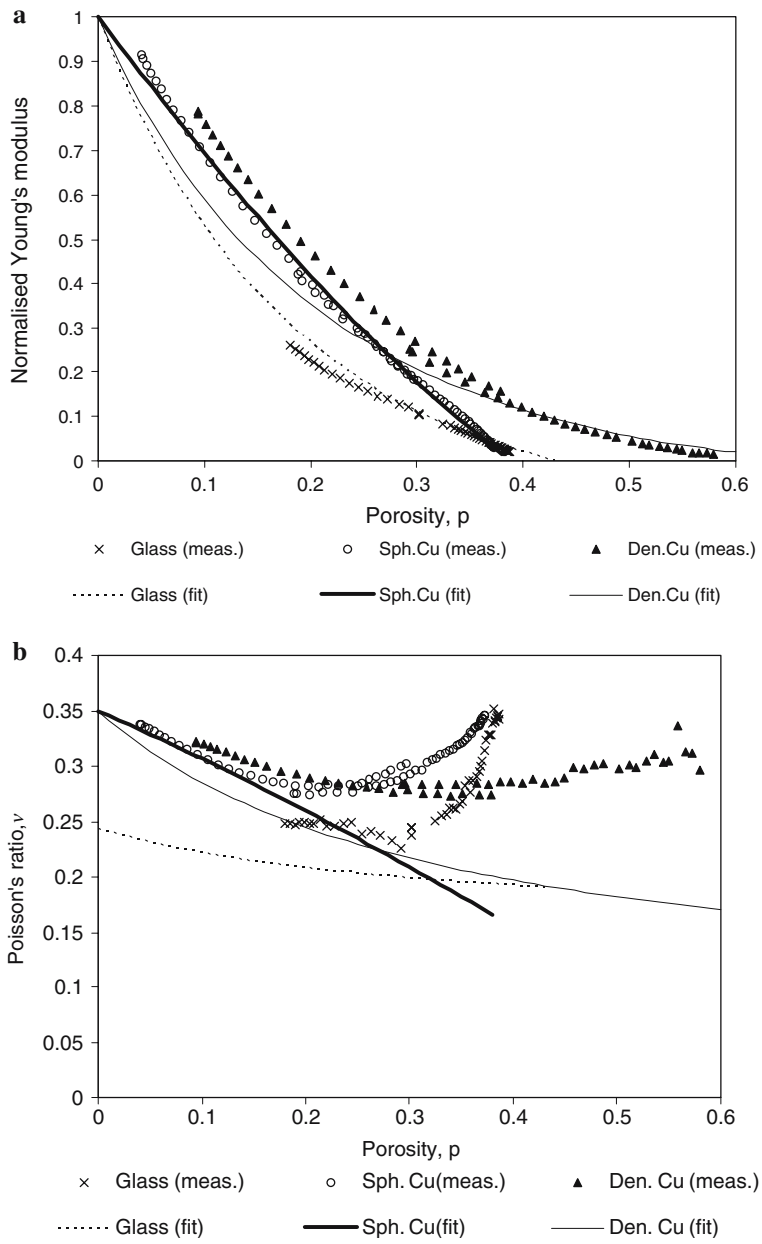

Fig. 3 Predictions of the Nielsen model (Eqs. 6, 7); see Table 1 for parameter values of β and p_c. (**a**) Normalised Young's modulus. (**b**) Poisson's ratio. Spheroidal glass: (×) measured, (- - - -) fitted. Spheroidal copper: (○) measured, (—) fitted. Dendritic copper: (▲) measured, (–) fitted

changes in microstructure, and hence β. This is a disadvantage common to many porous material models which describe shape using a single parameter [34, 46, 12, 58]. Potentially, this effect may be used to characterise changes in pore character with porosity, by obtaining a local rather than global value for β. However, it is necessary that the model accurately describes the experimental data to do so. Unfortunately, as exemplified by predictions for Poisson's ratio, and consideration of the boundary conditions for Poisson's ratio at p_c, the model of Nielsen is unable to meet this requirement for uniaxially compacted powders. Thus, discussion on the relative merits of finding an optimal value of the shape parameter at each porosity, is deferred until later (see subsection "Boccaccini et al. (1993)").

Zhao et al. (1989) (Isotropic model)

Zhao et al. [35] derived a model for the elastic properties of porous materials using the Mori–Tanaka method of homogenisation, with pores represented as ellipsoids. Two cases of interest to the current study were considered: (i) an elastically isotropic porous material, constructed of ellipsoids whose orientational distribution is random in three dimensions; and (ii) a transversely isotropic medium, containing ellipsoids

Table 1 Regression parameters for models of Kendall et al., Nielsen, Zhao et al. and Boccaccini et al. (Eqs. 5–7, 9–11, respectively)

Powder	Initial packing*		Kendall et al.	Nielsen		Zhao et al. α		Boccaccini et al.
	p_{tap}	p_a	Γ, (J m^{-2})	p_c	β	Isotropic	Transversely isotropic	α
Glass (spheroidal)	0.365	0.448	120	0.425	0.177	0.012	–	0.078
Aluminium (spheroidal)	0.402	0.514	1,340	0.445	0.437	0.031	0.075	0.188
Stainless steel (spheroidal)	0.379	0.469	1,420	0.421	0.462	0.011	0.029	0.110
Copper (spheroidal)	0.370	0.423	1,990	0.391	0.464	0.024	0.065	0.154
Copper (dendritic)	0.695	0.737	3,050	0.695*	0.206	0.026	0.076	0.197
Copper (irregular, US)	0.652	0.717	2,780	0.670	0.411	0.032	–	0.210
Copper (irregular, MM)	0.583	0.649	2,390	0.606	0.402	0.030	0.056	0.195
Iron (irregular)	0.625	0.698	3,830	0.652	0.327	0.029	–	0.173

Fitted values for additional experimental data presented in a companion paper [1] are also provided. * Indicates p_c was constrained to lie within bounds $p_{tap} < p_c < p_a$

* Experimentally measured quantities [65]

distributed with random orientations in two dimensions only. Discussion of the second case is deferred until ''Mechanistic pore-based models (Transversely isotropic)''. For an isotropic (completely random orientational) distribution of ellipsoidal pores, the following equations for Young's modulus, and Poisson's ratio result.

$$E = \frac{3E_{solid}(p-1)}{p(2\nu_{solid}-1)P_2(\nu_{solid},\alpha) - 2p(\nu_{solid}+1)Q_2(\nu_{solid},\alpha) + 3(p-1)} \tag{9}$$

$$\nu = \frac{p(2\nu_{solid}-1)P_2(\nu_{solid},\alpha) + p(\nu_{solid}+1)Q_2(\nu_{solid},\alpha) + 3\nu_{solid}(1-p)}{2p(\nu_{solid}+1)Q_2(\nu_{solid},\alpha) - p(2\nu_{solid}-1)P_2(\nu_{solid},\alpha) - 3(p-1)}. \tag{10}$$

Model parameters: $E = E(E_{solid}, \nu_{solid}, p, \alpha)$, and $\nu = \nu(\nu_{solid}, p, \alpha)$. $P_2(\nu_{solid}, \alpha)$ and $Q_2(\nu_{solid}, \alpha)$ are complicated functions of the Eshelby tensor that depend on the solid phase Poisson's ratio and the aspect ratio (α) of substitutional ellipsoids (for the sake of brevity, they are not provided here; please refer to the original reference [35] for further details). The aspect ratio, α, of the substitutional ellipsoids can vary within the range $0 < \alpha < \infty$, representing in the extremes disc and needle-shaped pores; $\alpha < 1$ represents an oblate ellipsoid, and $\alpha > 1$, a prolate ellipsoid, while $\alpha = 1$ is a sphere. For both Young's modulus and Poisson's ratio, increasing deviations from $\alpha = 1$ cause a more rapid decrease of the moduli with increasing porosity. $\alpha = 1$ (spherical pores) represents the stiffest possible system at a given porosity (a result common to other model predictions; see [1] for discussion). Deviations from $\alpha = 1$ reduce the stiffness, with oblate pores ($\alpha < 1$) having a much stronger effect than prolate pores ($\alpha > 1$). The reason for this behaviour becomes apparent when considering the extreme cases. A strongly oblate pore corresponds to a disc-like crack, for which a plane of solid phase material is discontinuous. Alternatively, the limiting case for a prolate pore is a needle-like crack, for which material is discontinuous along a single line only. Clearly, the latter case will have a lesser effect on elastic properties.

Both model equations depend on the solid phase Poisson's ratio, though the effect on Young's modulus only becomes significant for $\nu_{solid} > 0.4$ [65]. As with the model of Nielsen [40], higher values of ν_{solid} produce a falling characteristic of ν with p, while as ν_{solid} approaches zero, ν increases with p.

Boundary conditions: When $p = 0$: $E = E_{solid}$, $\nu = \nu_{solid}$. At $E = 0$: $p = p_c = 1$, and $\nu_c = \frac{(2\nu_{solid}-1)P_2(\nu_{solid},\alpha)+(\nu_{solid}+1)Q_2(\nu_{solid},\alpha)}{2(\nu_{solid}+1)Q_2(\nu_{solid},\alpha)-(2\nu_{solid}-1)P_2(\nu_{solid},\alpha)}$.

As with the model of Nielsen, the model of Zhao et al. yields the correct asymptotic limit for zero porosity. However, in this case, the existence of a critical porosity less than unity is not accommodated. Further, at $p = p_c = 1$, $\nu_c = 0.5$ does not hold in general [65]. As shown in the following, both have significant effects on the predictive ability of this model.

Application of the model (Eqs. 9, 10) to experimental data is illustrated in Fig. 4; best-fitting values of pore aspect ratio (obtained by minimisation of Eq. 8) are listed in Table 1. Regression values of α indicate strongly oblate pores, closely approximating disc-like cracks. A large contributor to the poor performance of this model when applied to uniaxially compacted powders is the inability of the model equations to admit vanishing stiffness before $p = p_c = 1$. Thus, the model must attempt to account for the observed porosity dependence of the experimental data, while satisfying both boundary conditions described above. While the upper boundary condition is met, model predictions of the lower boundary condition ($p_c = 1$)

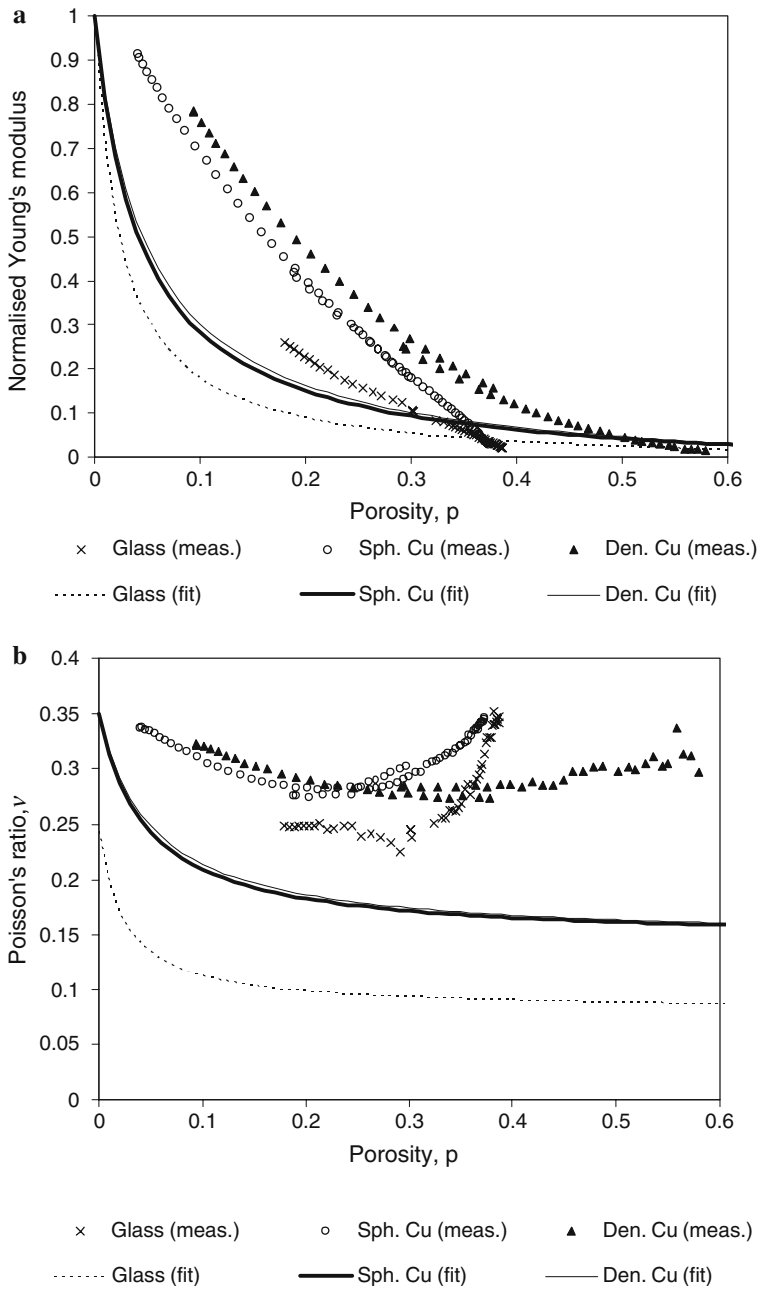

Fig. 4 Predictions of the model of Zhao et al. (Eqs. 9, 10); see Table 1 for parameter values of α. (**a**) Normalised Young's modulus. (**b**) Poisson's ratio. Spheroidal glass: (×) measured, (- - - -) fitted. Spheroidal copper: (○) measured, (—) fitted. Dendritic copper: (▲) measured, (–) fitted

deviates strongly from experimental data. Hence, it is the requirement for the model to smoothly asymptote to $p = 1$ (in a manner commensurate with its functional form), before the predicted stiffness can vanish (e.g. Fig. 4a), that leads to its poor predictive ability. In terms of the model, the region between $p = 1$ and the porosity at which each powder actually begins to exhibit elastic properties is effectively one of extremely high compliance. The relatively rapid transition between this region and the experimental data, is clearly unable to be accommodated by a model with the functional form suggested by Zhao and co-workers.

Boccaccini et al. (1993)

The model of Boccaccini et al. [61] also represents porosity by substitutional ellipsoids. The equation describing the model (Eq. 11) is based on the considerations of Mazilu and Ondracek [33] of an isolated ellipsoidal inclusion in a unit cell of matrix material

$$E = E_{\text{solid}}\left(1 - p^{2/3}\right)^{1.21\xi}. \tag{11}$$

where $\xi = \alpha^{1/3}\sqrt{1 + (\alpha^{-2} - 1)\cos^2\phi}$.

Model parameters: $E = E(E_{solid}, p, \alpha, \phi)$. α is the axial ratio of substitutional ellipsoids (pores); ϕ the angle between applied stress direction and the rotational axis of the substitutional ellipsoid, with $\phi = 54.7°$ ($\cos^2\phi = 0.3333$) representing a random (isotropic) ellipsoid distribution throughout the material [61]. Ellipsoids are characterised in the same manner as described previously: $\alpha = 1$ is a sphere; $\alpha > 1$ is a prolate ellipsoid; and $\alpha < 1$ an oblate ellipsoid. As with the model of Zhao et al. spherical pores produce the highest possible value of E for a given porosity. Likewise, oblate pores produce a stronger effect than prolate pores; though differences between the two cases are less pronounced [65]. Due to the symmetric nature of the $\cos^2(\phi)$ function, all values of ϕ will produce a curve within the bounds defined by those for which $0° < \phi < 90°$; however for values in the range $45° < \phi < 90°$, the effect of ϕ on E is not strong [65].

Boundary conditions: When $p = 0$: $E = E_{solid}$. At $E = 0$: $p = p_c = 1$. Note also that, $E \rightarrow 0$ as $\xi \rightarrow \infty$. However, given that $0 \leq \cos^2(\phi) \leq 1$, then $E \rightarrow 0$ in the limit as either $\alpha \rightarrow 0$, or $\alpha \rightarrow \infty$. An exception is when $\cos^2(\phi) = 1$, in which case $E \rightarrow 0$ only as $\alpha \rightarrow \infty$. Likewise, if $\cos^2(\phi) = 0$, then $E \rightarrow 0$ only if $\alpha \rightarrow 0$. Once again, this model appropriately satisfies the upper boundary condition, however it does not admit values of the critical porosity less than unity (except for limiting values of α).

Application of the model of Boccaccini et al. (Eq. 11) to experimental data is illustrated in Fig. 5. Both α and ϕ were used as regression parameters when generating the fitted curves. Initially, α was the only variable fitted, with ϕ fixed at 54.7° (an isotropic material). When α converged to a stable value, ϕ was also included as a fitting parameter. This method was adopted to determine whether Boccaccini's model could be used to indicate the presence of anisotropy. However, in all cases, no subsequent change in ϕ occurred. This indicates the model depends mainly on aspect ratio of the ellipsoidal pores is relatively insensitive to their presumed orientation.

Even though this model also assumes $p_c = 1$, it follows experimental data much better. This suggests the functional form of Eq. 11 is better able to cope with "transition" from the region of porosities in which the powders do not exhibit elastic properties. That only one modulus is calculated also reduces difficulties in determining an optimum fit to the data, although agreement with the copper powders is still relatively poor. While values of α obtained from this model seem more realistic in terms of expected sample microstructure, as with Nielsen's model, it does not discriminate between different compact microstructures

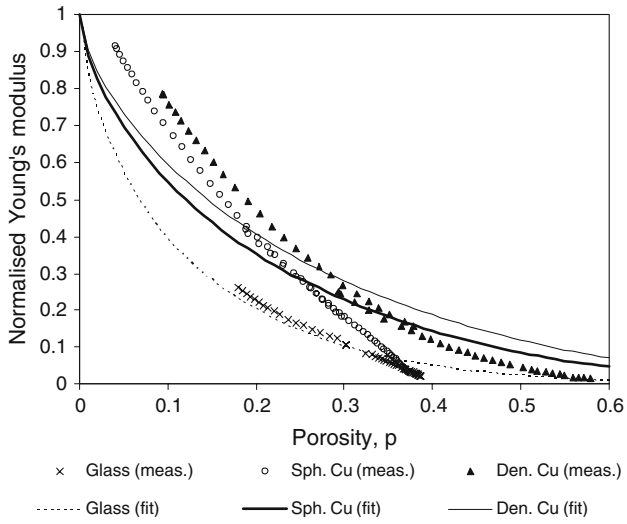

Fig. 5 Predictions of the model of Boccaccini et al. (Eq. 11) for Young's modulus of porous materials; see Table 1 for parameter values of α. Spheroidal glass: (×) measured, (- - - -) fitted. Spheroidal copper: (○) measured, (—) fitted. Dendritic copper: (▲) measured, (–) fitted

particularly well (Table 1). Again, this is most likely due to the inability of a single parameter to accommodate microstructural changes during powder compaction, i.e. α should be a function of porosity, not constant. To investigate this further, Eq. 11 was solved on a point-by-point basis, finding the optimal value of α at each porosity (see also [46]). Data for all powders discussed in [1] is provided to enable comparison between $\alpha(p)$ for a number of different powder compacts. The most basic result yielded by Fig. 6 is that α is not constant: the optimum pore aspect ratio changes

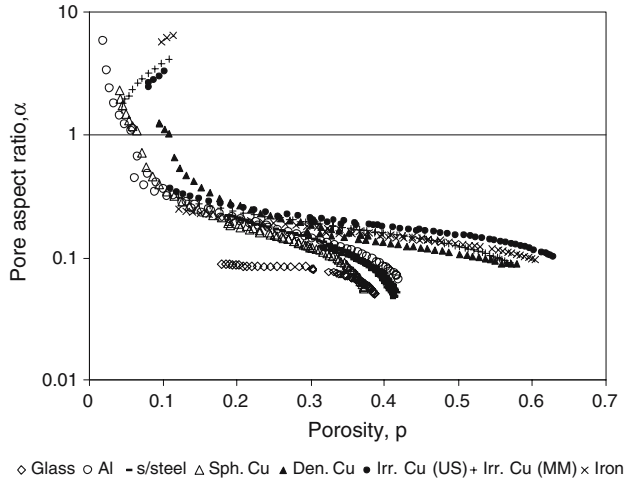

Fig. 6 Evolution of pore aspect ratio with porosity (calculated by solution of Eq. 11 on a point-by-point basis). (◇) spheroidal glass, (○) spheroidal aluminium, (-) spheroidal stainless steel, (△) spheroidal copper, (▲) dendritic copper, (♦) irregular copper (US), (+) irregular copper (MM), (×) irregular iron

during compaction. $\alpha(p)$ generally follows expected trends; at high porosities, the rugged powders are distinct from spheroidal powders. Further, the ductile and brittle spheroidal powders separate as porosity deceases, consistent with the diverging pore character expected due to different mechanisms of yield. Finally, $\alpha \rightarrow 1$ as $p \rightarrow 0$ consistent with evolution of pore character towards isolated spherical pores at low porosity.

To be of practical use though, values of α obtained by this procedure must be able to be unambiguously interpreted in terms of the material microstructure. However, by suitable selection of α (and ϕ), Eq. 11 can be made to pass through practically any individual point that lies beneath the line $E/E_{\text{solid}} = (1–p)$. Thus, any point within this parameter space can be specified using the model of Boccaccini et al. and a particular value of α (and ϕ). Similar comments hold for other models and their parameters as well, though their functional form may restrict access to a specific region of parameter space. However, as a local value of α is valid only for a single porosity, the elastic properties at other porosities cannot be predicted in the absence of independent information on the change of α with p. Thus, as described by Rice [58, 12], unless the physical interpretation of the shape parameter (α) can be assured, it essentially becomes an empirical parameter when fitted in such a manner, and its usefulness for microstructural characterisation is questionable in such a circumstance.

Arnold et al. (1996)

The model presented by Arnold et al. [62] is discussed here mainly because it is capable of producing the multi-valued porosity dependence of Poisson's ratio demonstrated by experimental measurements during uniaxial powder compaction [1]. The resulting equation is a combination of three separate models; two which describe the effect of porosity on bulk modulus (k), with one relation valid at high porosities and the other valid at low porosities. The two models are combined using a smoothing function, viz:

$$k(p) = (1 - s)k_{(\text{low } p)} + sk_{(\text{high } p)} \tag{12a}$$

$$s = \left[1 + e^{-a(p-b)}\right]^{-1} \tag{12b}$$

where $k_{(\text{low } p)}$, $k_{(\text{high } p)}$ are the bulk modulus models valid for low and high porosity, respectively; s is a smoothing function with empirical parameter values $a = 100$, and $b = 0.4$ recommended [61] for the smoothest join. $k_{(\text{low } p)}$ and $k_{(\text{high } p)}$ are:

$$k_{(\text{low } p)} = k_{\text{solid}} \frac{2(1 - 2\nu_{\text{solid}})(3 - 5p)(1 - p)}{2(3 - 5p)(1 - 2\nu_{\text{solid}}) + 3p(1 + \nu_{\text{solid}})} \tag{12c}$$

$$k_{(\text{high } p)} = k_{\text{solid}} \frac{2(1 - 2\nu_{\text{solid}})(1 - p)}{3(1 - \nu_{\text{solid}})}. \tag{12d}$$

Both models for bulk modulus assume spherical pores and do not have any adjustable parameters. The third model utilised is that of Boccaccini et al. [61] (Eq. 11) to describe the effect of porosity on Young's modulus. Arnold and co-workers combined these model equations for k and E using a well-known relation of isotropic linear elasticity (Eq. 13) to obtain Poisson's ratio as a function of porosity.

$$\nu(p) = 0.5 - \frac{E(p)}{6k(p)} \tag{13}$$

where $E(p)$ and $k(p)$ are given by Eqs. 11, 12a, respectively.

Model parameters: $\nu = \nu(\nu_{\text{solid}}, p, \alpha, \phi)$; α and ϕ are as defined for the model of Boccaccini et al. [61] (see subsection "Boccaccini et al. (1993)").

Boundary conditions: When $p = 0$: $s \rightarrow 0$, thus $k \rightarrow k_{(\text{low } p)} \rightarrow k_{\text{solid}}$. Thus, as $E = E_{\text{solid}}$ at $p = 0$ (see subsection "Boccaccini et al. (1993)"), $\nu \rightarrow \nu_{\text{solid}}$. At $E = 0$, there are three possibilities: (i) $p = p_c = 1$; (ii) $\alpha \rightarrow 0$; or (iii) $\alpha \rightarrow \infty$.

(i) If $p = 1$, then $s \rightarrow 1$ and $k \rightarrow k_{(\text{high } p)} \rightarrow 0$. With $k = 0$, and $E = 0$, ν is indeterminate; however, model plots indicate $\nu \rightarrow 0.5$ as $p \rightarrow 1$ [65], and hence $p = 1$ is again the critical porosity for this model. For cases (ii) when $\alpha \rightarrow 0$, and (iii) $\alpha \rightarrow \infty$; $\nu \rightarrow 0.5$, assuming k remains finite (given it is not a function of either α, or ϕ).

Model predictions: Unlike the previous models for Poisson's ratio, the model of Arnold and co-workers can accommodate both a rising and falling characteristic for ν as a function of p (for a given value of ν_{solid}) [65]. This dual character arises from the two different models used for bulk modulus; the low porosity model (Eq. 12c) potentially allows ν to decrease with p, while the high porosity model for k (Eq. 12d) accounts for the branch where ν increases with p [65]. Changing the pore aspect ratio in the model for Young's modulus (Eq. 11) shifts the $\nu(p)$ curve towards $\nu = 0.5$. Again, oblate pores have a stronger effect than prolate pores [65].

Model predictions are compared with experimental data in Fig. 7. Values of Young's modulus were calculated using parameters which provide the best fit to Eq. 11 as described previously (see subsection ''Boccaccini et al. (1993)''). The resulting predictions of Poisson's ratio are poor indicators of measured data, being substantially higher in all cases. This is most likely because only part of the model (the equation for Young's modulus) considers pore character: predictions of bulk modulus are based on models assuming spherical pores. As discussed above (see subsections ''Zhao et al. (1989) (Isotropic model)'' and ''Boccaccini et al. (1993)'') and elsewhere [1], spherical pores generally provide the stiffest possible system at a given porosity. While the prediction of E accounts for reduced stiffness due to pore shapes other than spherical, k is fixed to be the stiffest possible (spherical pores). Hence, the term $E/(6k)$ is presumably smaller than would be the case if both accounted for non-spherical pores, increasing ν towards 0.5. Again, the constraint imposed by the lower boundary condition $p_c = 1$ (as discussed in subsection ''Zhao et al. (1989) (Isotrophic model)'') may also contribute to the poor predictive ability of the model by Arnold et al. when applied to description of $\nu(p)$ for powders undergoing uniaxial compaction.

Mechanistic pore-based models (Transversely isotropic)

In the model of Zhao and co-workers [35] discussed previously (see subsection ''Zhao et al. (1989) (Isotropic model)''), an isotropic porous material was modelled by considering a random distribution of ellipsoids in three dimensions. In addition, Zhao and co-workers also presented a model appropriate to transversely isotropic materials by restricting the orientational distribution of the ellipsoidal pores to be random in two rather than three dimensions. Equations for five moduli (E_a, E_r, μ_r, μ_a, ν_a) resulted, as is required to completely describe the elastic properties of a transversely isotropic medium (Eqs. 14–18).

$$E_r = \frac{E_{solid}(1-p)}{(1-p)+pP_{11}(\nu_{solid},\alpha)} \tag{14}$$

$$E_a = \frac{E_{solid}(1-p)}{(1-p)+pP_{33}(\nu_{solid},\alpha)} \tag{15}$$

$$\mu_r = \frac{\mu_{solid}(1-p)}{(1-p)+pP_{12}(\nu_{solid},\alpha)} \tag{16}$$

$$\mu_a = \frac{\mu_{solid}(1-p)}{(1-p)+pP_{13}(\nu_{solid},\alpha)} \tag{17}$$

$$\nu_a = \frac{(1-p)+pP_{31}(\nu_{solid},\alpha)}{(1-p)+pP_{33}(\nu_{solid},\alpha)}. \tag{18}$$

Model parameters: $E_a = E_a(E_{solid}, \nu_{solid}, p, \alpha)$; $E_r = E_r(E_{solid}, \nu_{solid}, p, \alpha)$; $\mu_r = \mu_r(\mu_{solid}, \nu_{solid}, p, \alpha)$; $\mu_a = \mu_a(\mu_{solid}, \nu_{solid}, p, \alpha)$; $\nu_a = \nu_a(\nu_{solid}, p, \alpha)$. $P_{11}(\nu_{solid}, \alpha)$, $P_{12}(\nu_{solid}, \alpha)$, $P_{33}(\nu_{solid}, \alpha)$, $P_{13}(\nu_{solid}, \alpha)$, and $P_{31}(\nu_{solid}, \alpha)$ are functions of the Eshelby tensor, depending on the solid phase Poisson's ratio and the aspect ratio (α) of substitutional ellipsoids (see [35] for details).

Boundary conditions: At $p = 0$, $\mu_a = \mu_r = \mu_{solid}$; $E_a = E_r = E_{solid}$; $\nu_a = \nu_{solid}$. $E_a = E_r = 0$, and $\mu_a = \mu_r = 0$ only for $p = p_c = 1$, and $\nu_{a,c} = \frac{P_{31}(\nu_{solid},\alpha)}{P_{33}(\nu_{solid},\alpha)}$.

As with the isotropic model (see subsection ''Zhao et al. (1989) (Isotropic model)''), this model also satisfies the correct upper boundary condition, but does not admit a critical porosity less than unity. Again, oblate pores have more pronounced effects on the elastic moduli than prolate pores. However, in contrast to previous models, it is now possible for a pore shape other than spherical to have the highest Young's modulus at a given porosity [65]. For shear modulus, however, spherical pores still represent the stiffest possible pore character.

Predictive ability of the transversely isotropic model of Zhao et al. (Eqs. 14–18) was evaluated by comparison with the experimental data provided elsewhere

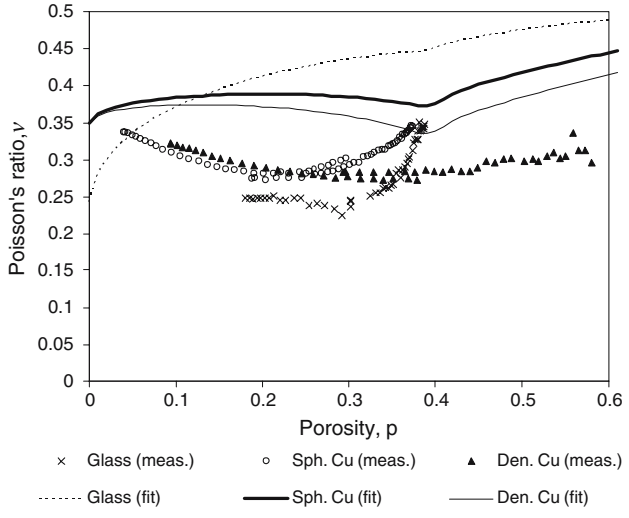

Fig. 7 Predictions of Poisson's ratio according to the model of Arnold et al. Spheroidal glass: (×) measured, (- - - -) fitted. Spheroidal copper: (○) measured, (—) fitted. Dendritic copper: (▲) measured, (–) fitted

[2]. The lack of experimental data on C_{13} limits rigorous comparison between model predictions and experimental data to μ_a and μ_r only. Although it is possible to obtain estimates of the remaining three moduli (E_r, E_a, ν_a) by use of the Saint-Venant approximation [2], an alternative is to re-cast Eqs. 14–18 to predict the components of the stiffness matrix (C_{ij}) for a transversely isotropic material. This method was preferred as it maximises use of experimental data. As with the isotropic model, the aspect ratio, α of the substitutional ellipsoids was used as a regression parameter by minimising an equation analogous to Eq. 8 containing terms for C_{11}, C_{12}, C_{33}, and C_{44}. The predicted values were then re-transformed to the engineering moduli (E_r, E_a, μ_r, μ_a, ν_r, ν_a), for comparison with estimated values from experimental data. As a result, the experimental data for Young's modulus and Poisson's ratio should be taken as a guide only. This is not considered to be significant in the present case, as the resulting model predictions are not of sufficient quality. Regardless, the model fits can be still be explicitly compared with the data for shear modulus, as these points correspond to direct experimental measurements. This slightly convoluted procedure was preferred to discussing the model in terms of C_{ij}, as the engineering moduli are easily interpreted, and are more readily compared with the predictions of the isotropic moduli discussed previously. Representative results are provided in Fig. 8 for the spheroidal and dendritic copper powders. The regressed values of the pore aspect ratio are provided in Table 1, along with the equivalent values for the isotropic model of Zhao and co-workers.

The predictive ability of this model is still quite modest, though improved relative to the isotropic model. Predictions for the shear moduli agree best with experimental data, though again, these seem hampered by the requirement of retaining finite material stiffness for all porosities less than unity. This appears to be a significant disadvantage of the modelling approach used by Zhao and co-workers. Furthermore, the large difference between Young's modulus for the radial and axial planes is not replicated in the data. Similar comments hold for Poisson's ratio.

In total, these results indicate the assumed pore anisotropy between the axial and radial directions is too strong. For this model, the differences between the two planes is obtained by randomly orienting the ellipsoids in two dimensions, but constraining their axis of symmetry to lie within the plane of isotropy. Zhao and co-workers also present models in which the symmetry axes of the ellipsoids are distributed at an angle to the transverse plane normal. Solutions for sine and cosine distributions were presented (a uniform distribution results in the isotropic model discussed earlier). Both distributions provide a more gradual transition between pore orientation between the axial and radial planes, which will reduce the difference between moduli predictions between axial and radial planes. However, these models are not considered here as it is would be difficult to provide experimental justification for such pore distributions, certainly for the case of powder compaction. Further, it is unlikely that the distributions considered by Zhao et al. will produce accurate model predictions, as it is predicted that either the shear modulus of the radial plane exceeds that of the axial plane (sine distribution); or alternatively, Young's modulus for the radial plane is greater than the axial plane (cosine distribution). This situation contradicts the trends of the experimental data, for which both Young's modulus and shear modulus are higher in the axial plane.

As may be expected, there is little correspondence between the best-fitting values of pore aspect ratio for the isotropic and transversely isotropic models, with α for the transversely isotropic model approximately twice that for complete isotropy. This is attributed mainly to the poor fit of the isotropic model. Overall, the model for transverse isotropy still has very limited success for the description of the elastic properties of compacted powders, particularly for Young's modulus and Poisson's ratio. However, it is felt that the improvement relative to the model assuming complete isotropy illustrates the need to account for elastic anisotropy in model development, especially when considered that, with the exception of the orientational distribution of the substitutional ellipsoids, both models have the same underlying assumptions.

Geometric pore-based models

Minimum solid area models (Rice 1998)

Minimum solid area (MSA) models belong to the category of geometric models, which assume macroscopic elastic response is related to the load-bearing area of the solid phase material. The key assumption in MSA models is that normalised Young's modulus equals normalised minimum solid area of the porous material [47, 48, 58, 12] (see section ''Approaches to modelling'' under subsection ''Geometric pore-based models''). Models discussed by Rice [12] consider the change in MSA with porosity for idealised microstructures. Many different microstructures were considered, including regular packing of spheres in a

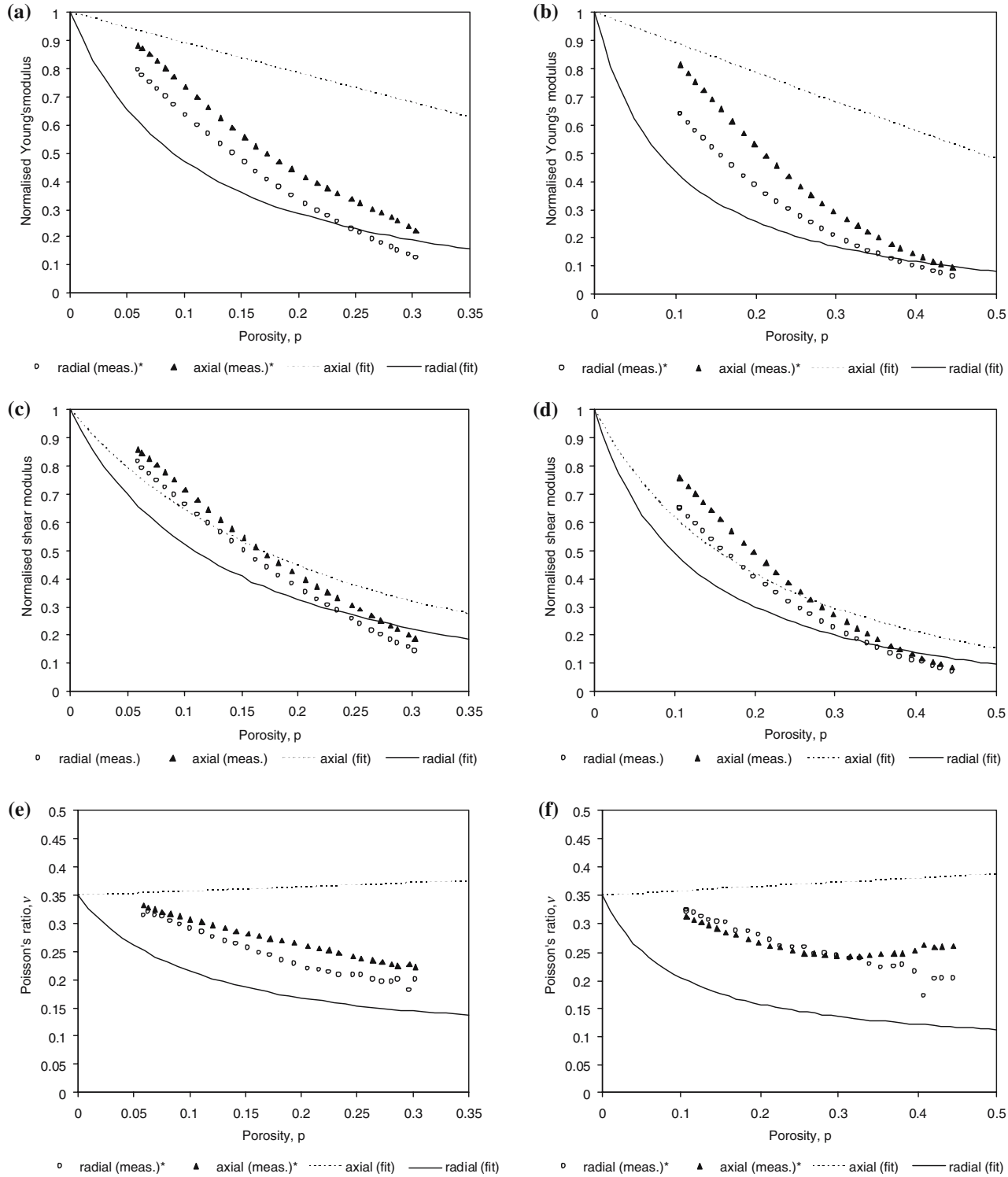

Fig. 8 Transversely isotropic model for elastic properties according to Zhao et al. see Eqs. 14–18. Model predictions are compared with data for spheroidal copper powder (**a**), (**c**), (**e**); and dendritic copper powder (**b**), (**d**), (**f**). (- - - -) Fits to model predictions for the axial plane; (–) fits of predicted moduli for the radial plane. (▲) Experimental data for axial plane; (○) experimental data for the radial plane. * Denotes moduli estimated by adopting the Saint-Venant approximation

void matrix, and regular packings of pores (spheres, cylinders, etc.) in a solid phase matrix. Some advantages, and potential disadvantages of this approach were discussed in section ''Approaches to modelling'' under subsection ''Geometric pore-based models''.

Possibly the most attractive feature of these models is that changes in sample microstructure with porosity are incorporated in a physically realistic manner. As a specific example, consider a microstructure composed initially of a simple cubic packing of identical spheres. This microstructure can be simplified by considering a representative sphere bounded by a cube (unit cell). Densification of the packing can be considered conceptually by uniformly shrinking the cube so that it intersects the sphere. To ensure conservation of mass, ''truncated'' solid phase material is evenly redistributed over the free surface within the cube such that the volume of solid phase material inside the cube always equals the volume of the initial sphere [12]. The area of intersection between cube faces and the sphere will be the smallest cross-sectional area for the packing, and hence is the minimum solid area for this microstructure. Other microstructures (e.g. spherical pores in a solid matrix) can be considered using the same basic approach. Thus, the general term ''MSA models'' in fact describes a suite of models; each is constructed in a similar manner, but differ in the initial microstructure considered.

A strong positive of MSA models is that both boundary conditions are properly satisfied. For example, at porosities slightly higher than the initial simple cubic packing, NMSA and hence E/E_{solid} is zero. Alternatively, at $p = 0$, the initially spherical particle has deformed into a cube so NMSA = $E/E_{solid} = 1$. However, the manner in which MSA models incorporate microstructural changes entails certain assumptions of material behaviour. For instance, in the model based on cubic packings of spheres, as porosity is reduced it is assumed the ''truncated'' material (in the contact region) is uniformly distributed over the non-contacting surfaces of the particle. This assumption makes the model most applicable to sintered microstructures and possibly compaction of ductile powder materials. Micrographs of particles recovered from compacts of spheroidal powders at various stages throughout compaction are presented elsewhere [65]. For ductile powders, large flat deformation faces were found to develop at inter-particle contacts. Thus, MSA models based on packings of solid spheres should provide a reasonable description of the evolving microstructure within a compact of ductile spheroidal particles. The analogy will not be exact however, as material displaced by plastic flow will remain in the contact region rather than being uniformly distributed over the remaining surfaces. Similarly, for sintered powders, solid phase material will diffuse to the contact region to form ''necks'' between particles (e.g. [66]). In both cases, MSA models will predict a slightly higher compliance, as the calculated areas of contact will be less. Still, it is clear that this approach to modelling better replicates the compaction-induced changes in pore character than models which idealise the pore space by ellipsoids. Certainly, the physical link to the assumed microstructure is much stronger. Comparison between experimental data and predictions of some MSA models is presented in Fig. 9.

The porosity at which spheroidal powder compacts first demonstrate measurable elastic properties lies intermediate between predictions of MSA models for simple cubic and rhombohedral sphere packings. This is consistent with the expectation that neither regular packing accurately replicates real particle packings. With reducing porosity, the dependence of normalised Young's modulus for the spheroidal copper powder rapidly approaches the model microstructure for a simple cubic packing of spheres. Significantly though, the rate at which Young's modulus for the spheroidal copper powder increases with reducing porosity, most closely matches the porosity dependence of the rhombohedral model. This indicates the higher coordination number of the rhombohedral packing (initially 12) is more appropriate than the simple cubic packing (initially four). Micrographs of particles recovered from uniaxial compacts [65] generally support this.

With reducing porosity, the dependence of Young's modulus for the spheroidal glass powder diverges from the spheroidal copper. This result is attributed to

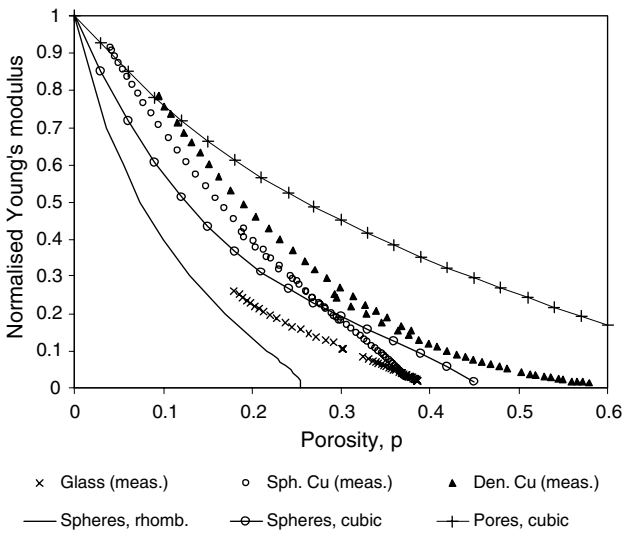

Fig. 9 Comparison of three MSA models with experimental data. MSA models: (–) rhombohedral packing of solid spheres, (—○—) simple cubic packing of solid spheres, (—┼—) simple cubic packing of spherical pores. Experimental data: (×) spheroidal glass, (○) spheroidal copper, (▲) dendritic copper

differences in contact geometry, rather than packing, and is indicative of differences in solid phase yield mechanisms. Micrographs of particles recovered from the glass compacts [65], illustrate that compaction of brittle powders produces angular fracture debris, rather than the flat deformation faces observed on ductile particles. Clearly, this represents a significant departure from the contact geometry assumed by MSA models, illustrating the importance of correctly accounting for differences in the evolution of porosity according to solid phase yield behaviour. A further example of this is furnished by the dendritic and spheroidal copper powders at the lowest porosities, both of which asymptote towards the MSA model based on cubic stacking of spherical pores. This indicates that initial differences due to the convex features of porosity associated with sphere packings, and the irregular pore geometry of rugged particle packings are gradually reduced as compaction proceeds. For both, the pore spaces apparently take on an increasingly spherical nature with compaction. In all, the MSA approach is remarkably successful; particularly given its simple physical basis. It is felt much of this success owes to incorporating microstructural changes that are physically realistic, particularly for ductile materials.

Wang (1984)

The final model for isotropic elastic moduli considered here is due to Wang [4]. This model is also representative of geometrically based load-bearing area models. Again, a simple cubic packing of identical spheres is assumed, and the densification process is considered to occur in the manner described in ''Minimum solid area models (Rice 1998)''. However, in contrast to the MSA models described by Rice [12], elastic deformation of the whole particle (truncated sphere) is considered, rather than assuming the contact area dominates. Predictions of this approach are compared with experimental data in Fig. 10, along with two modifications to account for effects of non-ideal packing. These account for mis-alignment of the applied stress with <1 0 0>, which introduces a shearing effect (''imperfect''), and additionally, a ''hinge'' effect at the particle contact. Unfortunately, these modifications are not entirely rigorous, as it is assumed that the normalised Young's modulus and shear modulus have the same porosity dependence. By Eqs. 1–3, this is equivalent to assuming that Poisson's ratio is constant at the solid phase value throughout.

The difference between the models of Wang illustrates the importance of non-ideal alignment for models based on regular packings. Also of note is the

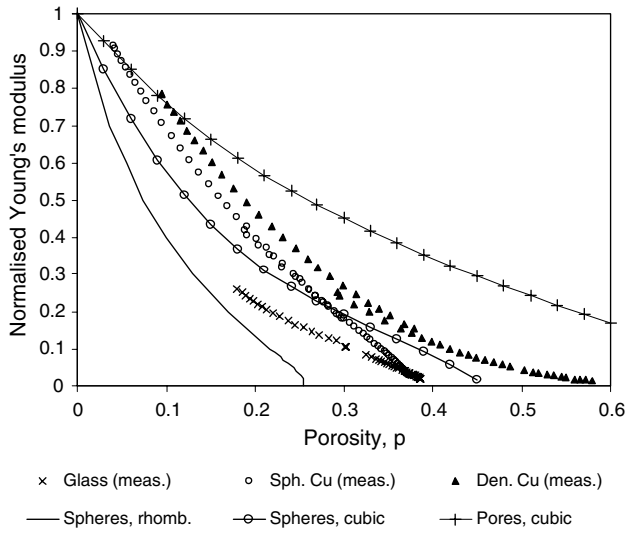

Fig. 10 Comparison between model predictions of Wang [4] and experimental data. Experimental data: (×) spheroidal glass, (○) spheroidal copper, (▲) dendritic copper. Wang models: (—○—) ''perfect'' simple cubic packing of solid spheres, (—┼—) ''imperfect'' packing, (—) ''hinge'' effect. (- ● -) MSA model predictions for a simple cubic packing of solid spheres is also shown

difference between the models assuming elastic deformation is localised at the contact area (MSA model) compared to the ideal model of Wang that considers deformation distributed throughout the bulk of the particle. With increasing densification towards zero porosity, the MSA model assumption of localised deformation loses validity, as the elastic straining must eventually be uniformly distributed throughout the solid phase material. This may not be of practical importance however, as all model predictions converge towards the solid phase value at zero porosity.

Discussion

Several models that have previously been proposed to account for the porosity dependence of elastic properties in granular and porous materials were compared with experimental results on the evolving elastic properties of powders during uniaxial compaction. The list of models selected for study is by no means exhaustive; those chosen were considered representative of the basic approaches to model building: particle-based, and pore-based (comprising of mechanistic and geometric models). Preference was given to models which consider sample microstructure, either through a shape parameter, or are constructed considering a definite microstructure. Model predictions were compared to experimental data on evolving

elastic moduli of powders during compaction. The data considered spans an appreciable porosity range, and encompasses a wide range of powder morphologies, and material behaviour (yield mechanism, solid phase elastic properties). When evaluating the relative merits of each model, attention was focussed on identifying correct model behaviour in terms of evolving microstructure, rather than the ability to follow measured data. As such, statistics to evaluate goodness-of-fit were not considered.

A selection of attributes considered essential for accurate prediction of elastic moduli of a completely isotropic material are listed in Table 2, along with an indication of whether each individual model possesses these features. Similar attributes are also desirable in models accounting for elastic anisotropy, however, only one of the models considered here had this capability.

When considered purely in terms of the ability to match experimental observations, the model of Nielsen [40] appears most successful. However, as discussed previously, the shape parameter of this model (β) does not have a clear interpretation in terms of material microstructure, certainly not to the extent that it can be directly measured. This is an important deficiency for this model and many others. While it is acknowledged that it is a difficult task to characterise the microstructure, particularly at high porosity, it is felt this problem must be addressed. Further, the evolution of sample microstructure, i.e. $\beta(p)$, also needs to be incorporated, either implicitly within the model, or by use of a dedicated secondary model. It is important however, that any descriptors used have a clear link to the sample microstructure. As discussed by Rice [58, 12], without clear physical interpretation, fitted parameters essentially become empirical. Care must be taken to ensure the parameter that accounts for shape remains consistent with its initial function, and does not incorporate additional effects not included in the formulation of the original model. An example of this is furnished by application of the model of Kendall et al. [8] to predict Young's modulus during uniaxial powder compaction. If the interface energy (Γ) is used as a regression parameter (see subsection ''Kendall et al. (1987)''), effects on compact stiffness due to permanent deformation of powder particles are inevitably included in its calculated value: Γ assumes higher values to account for the additional bonding effects of powder compaction. This arises because the original model only considered elastic deformation; and while the resulting model fits are quite acceptable, the parameter values are unrealistic to the feature they are to describe.

Pore aspect ratio (α) is affected by similar issues when used as a fitting parameter: model deficiencies and the violation of model assumptions may be obscured by α assuming values which are inconsistent with the sample microstructure. Particular among these is that most mechanistic models only incorporate pore elongation when considering effects that reduce material stiffness: the contribution of pore irregularity is neglected. This omission is at least part of the reason strongly oblate pores are often predicted, as required to account for the reduced stiffness due to pore irregularity. However, even if effects of pore irregularity are included, accurate description of the elastic properties over a range of porosities is still unlikely to result, as the microstructure inevitably changes with porosity. The importance of accounting for a *changing* microstructure is illustrated by comparing the MSA models

Table 2 Comparison between features of the models considered in section ''Evaluation of specific models'' under subsections ''Particle-based models'' to ''Mechanistic pore-based models (Transversely isotropic)'' (Y) denotes the model possesses this feature, (N) indicates it does not

Model	E and ν	Analytic basis	Asymptotic behaviour					Pore shape	Micro-structural interpretation	Micro-structural changes
			At $p = 0$		At $p = p_c$		$p_c < 1$			
			$E=E_{solid}$	$\nu=\nu_{solid}$	$E=0$	$\nu=0.5$				
Kendall et al. [8]	N	Y	N	–	Y	–	N	N	–	N
Nielsen [40]	Y	Y	Y	Y	Y	N	Y	Y	N	N
Zhao et al. [35]	Y	Y	Y	Y	Y	N	N	Y	N	N
Boccaccini et al. [61]	N	Y	Y	–	Y	–	N	Y	N	N
Arnold et al. [62]	Y	Y	Y	Y	Y	Y	N	Y	N	N
MSA models Rice [12]	N	Y	Y	–	Y	–	Y	–*	–	Y
Wang [4] analytic	N	Y	Y	–	Y	–	Y	–*	–	Y

Note: *Pore shape* refers to whether the model has a quantitative parameter to describe pore character. *Microstructural interpretation* denotes a clear interpretation of the parameter is possible (i.e. can be measured from the pore structure)

* Pore shape is included implicitly during model development rather than appearing as quantitative model parameter

and that of Wang [4], to the model suggested by Kendall et al. [8]. Each of these models is based on regular packing of identical spherical particles. However, while the MSA models and the approach of Wang [4] both consider changes in microstructure resulting from permanent deformation of the solid phase material as porosity is reduced, the model of Kendall and co-workers does not. As discussed previously, application of Kendall's model to situations involving permanent deformation of the particles then results in unrealistic values of the model parameters.

Despite the positives of their ability to incorporate microstructural evolution, the geometric models of Wang [4] and Rice [12] still remain somewhat limited. Model predictions for ductile spheroidal particles are generally quite good, and could possibly be improved further by incorporating evolution from sphere packings to pore stacked geometries as porosity is decreased. However, as results for the spheroidal glass powder illustrate, it is somewhat more challenging to account for microstructural changes during compaction of a brittle powder. Similar comments hold for a rugged powder (dendritic copper); it is not clear how a microstructure appropriate to such a powder would evolve with porosity, nor even how it would be defined initially. That is, a given model lacks the ability to be adapted to a new microstructure. For each different microstructural evolution a new model must be formulated. This is particularly challenging for powders whose constituent particles differ significantly from simple geometric shapes.

A limitation common to many mechanistic models is the inability to account for vanishing stiffness at porosities less than unity (e.g. the isotropic model of Zhao et al. [35]), which is related to the more general problem of not properly accounting for changes in sample microstructure with porosity. Indeed, the results discussed above suggest p_c is the most important model parameter aside from porosity itself. This is supported by recent results [67] which demonstrate that individual MSA model predictions can be brought into close coincidence if porosity is normalised by p_c, i.e. direct substitution of p with p/p_c. However, many mechanistic models will be rendered invalid by a similar substitution as the magnitude of mechanical fields, and hence the predicted response, depends directly on porosity (which is not equivalent to p/p_c) [12]. Complete re-formulation of the model to incorporate p_c would be required. Even so, the worth of this is questionable given that most mechanistic models are an extension of models assuming non-interacting inclusions. Interaction is approximated by considering surrounding pores modifying either the effective properties of a matrix or the effective mechanical field. But this can not hold at the highest porosities (close to the critical porosity) when there is extensive pore interconnection, as the stress and strain fields within the material will be highly heterogeneous. For this situation, the relative placement of pores will be critical; however, homogenisation approaches ignore this, effectively pores can be placed anywhere.

Thus, in terms of the ability to predict the elastic moduli of a given powder during compaction, with information known only on the solid phase material properties, yield mechanism, starting particle shape, and compact microstructure at various stages throughout compaction (e.g. sectioned images), none of the models is entirely successful. It is still not possible to accurately predict the elastic properties at a given porosity purely on this basis. The main reason for this is the inability to extract information from the sample microstructure that can be incorporated into such a model. The models either incorporate a parameter to account for an unknown microstructure (which is often used in an empirical way), or assume a particular (often highly idealised) microstructure. It is felt that useful models for describing the elastic properties of granular materials during compaction need to combine these aspects of the mechanistic and geometric modelling approaches. That is, combine the adaptive ability of mechanistic models with the ability of geometric models to describe changing microstructure with porosity.

In summary, for accurate prediction of elastic properties of powders during compaction, it is considered necessary that a model has the ability to:

- Predict all elastic moduli (complete specification of C_{ij}).
- Cover the entire porosity range ($0 \le p \le p_c$).
- Satisfy both boundary conditions (at zero porosity and the critical porosity).
- Describe changing microstructure with porosity.
- Be adaptive to different starting microstructures.
- Accommodate solid phase materials with different yield mechanisms (ductile and brittle).
- Describe elastic anisotropy.

Conclusions

Models have previously been published which describe the variation of elastic properties as a function of porosity in porous or granular materials. Representative samples have been chosen for detailed comparison

with experimental data obtained during the compaction of powders. Both ductile and brittle powders were considered, as was starting powder particle shape (hence pore character). Models considered were *Particle Based Models*, typified by that due to Kendall and co-workers, *Mechanistic Pore-Based Models* (*Isotropic*), typified by that due to Nielsen, Zhao and co-workers (for isotropic case), Boccaccini and co-workers, Arnold and co-workers, *Mechanistic Pore-Based Models* (*Transversely isotropic*) due to Zhao and co-workers, and *Geometric Pore-Based Models*, typified by the MSA models of Rice and the geometrically based load bearing area model of Wang.

The particle-based model of Kendall predicted a functional dependence of Young's modulus with porosity which agreed reasonably well with experiment, provided the surface energy parameter (Γ) was used as a fitting parameter rather than a physically based material constant. Agreement was best with irregular ductile copper powder and worst with brittle spherical glass powder. However, this model only provides information about one elastic modulus and therefore provides an incomplete description of the elastic response.

Of the isotropic pore-based models, that due to Nielsen gave the best agreement with experiment. However, with the one exception of the Arnold model, all models in this class showed a monotonically decreasing value for Poisson's ratio as porosity increased. This contrasts with experiment which shows that a minimum value occurs in Poisson's ratio at an intermediate value of porosity.

The transversely isotropic pore-based model of Zhao showed some qualitative agreement when compared with measured values of elastic properties during uniaxial compaction. The model correctly predicted that both Young's modulus and Poisson's ratio in the axial plane were larger than equivalent parameters in the radial plane, but the model overpredicted the difference between axial and radial values. Predicted values for shear modulus were much more accurate.

Of the geometric pore-based models considered in detail, that of Rice based on minimum solid area gave the closest agreement in terms of functional dependence of elastic properties on porosity. For Young's modulus, the experimental results fell between predictions of the MSA models for rhombohedral sphere packings and cubic packing of spherical pores, suggesting the need to consider a transition in microstructure during compaction. Again, this model class only encompasses a single elastic modulus and therefore does not provide a complete description of elastic behaviour.

Acknowledgement The authors gratefully acknowledge scholarship support for MLH through the Australian Research Council Small Grants Scheme.

References

1. Hentschel ML, Page NW Elastic properties of powders during compaction. Part 1: Pseudo-isotropic moduli. J Mater Sci (accepted)
2. Hentschel ML, Page NW Elastic properties of powders during compaction. Part 2: Elastic anisotropy. J Mater Sci (accepted)
3. Dean EA, Lopez JA (1983) J Am Ceram Soc 66:366
4. Wang JC (1984) J Mater Sci 19:801
5. Timoshenko SP, Goodier JN (1970) Theory of elasticity, 3rd edn. McGraw-Hill, Singapore
6. Duffy J, Mindlin RD (1957) J Appl Mech 24:585
7. Deresiewicz H (1958) Adv Appl Mech 5:233
8. Kendall K, Alford NMCN, Birchall JD (1987) Proc R Soc Lond A 412:269
9. Iida K (1939) Bull Earthq Res Inst 17:783
10. Takahashi T, Satô Y (1949) Bull Earthq Res Inst Japan 27:11
11. Duffy J (1959) Trans ASME J Appl Mech 26:88
12. Rice RW (1998) Porosity of ceramics. Marcel Dekker, New York
13. Dantu P (1957) Proceedings of the 4th International Conference on Soil Mechanics and Foundations Engineering, vol 1. p 144
14. Liu C-H, Nagel SR, Schecter DA, Coppersmith SN, Majumdar S, Narayan O, Witten TA (1995) Science 269:513
15. Brandt H (1955) J Appl Mech 22:479
16. Digby PJ (1981) J Appl Mech Trans ASME 48:803
17. Walton K (1987) J Mech Phys Solids 35:213
18. Emeriault F, Chang CS (1997) J Eng Mech 123:1289
19. Endres AL (1990) J Appl Mech Trans ASME 57:330
20. Chang CS, Chao SJ, Chang Y (1995) Int J Solids Struct 32:1989
21. Chang CS, Liao CL (1994) Appl Mech Rev 47:S197
22. Dong J-J, Pan Y-W (1999) Int J Num Anal Meth Geomech 23:1075
23. Bathurst RJ, Rothenburg L (1988) J Appl Mech Trans ASME 55:17
24. Misra A, Chang CS (1993) Int J Solids Struct 30:2547
25. Kruyt NP, Rothenburg L (2001) Int J Solids Struct 38:4879
26. Kruyt NP, Rothenburg L (1998) Int J Eng Sci 36:1127
27. Mackenzie JK (1950) Proc Phys Soc Lond 63B:2
28. Hashin Z (1962) J Appl Mech Trans ASME 29:143
29. Zimmerman RW (1991) Mech Mater 12:17
30. Sayers CM, Smith RL (1982) Ultrasonics 20:201
31. Rossi RC (1968) J Am Ceram Soc 51:433
32. Kreher W, Ranachowski J, Rejmund F (1977) Ultrasonics 14:70
33. Mazilu P, Ondracek G (1990) In: Herrmann KP Olesiak ZS (eds) Thermal effects in fracture of multiphase materials. Proceedings of the Euromech Colloquium 255, Oct. 31–Nov. 2, 1989. Panderburn, FRG, pp 214–226. Springer-Verlag. Berlin. (1990)
34. Dean EA (1983) J Am Ceram Soc 66:847
35. Zhao YH, Tandon GP, Weng GJ (1989) Acta Mech 76:105
36. Kachanov M, Tsukrov I, Shafiro B (1994) Appl Mech Rev 47:151
37. Eshelby JD (1957) Proc R Soc Lond A 241:367
38. Bert CW (1985) J Mater Sci 20:2220
39. Nielsen LF (1984) J Am Ceram Soc 67:93

40. Nielsen LF (1982) Mater Sci Eng 52:39
41. Hill R (1963) J Mech Phys Solids 11:357
42. Hashin Z, Shtrikman S (1963) J Mech Phys Solids 11:127
43. Balendran B, Nemat-Nasser S (1995) J Mech Phys Solids 43:1825
44. Nemat-Nasser S, Hori M (1993) Micromechanics: overall properties of heterogeneous materials. Elsevier, Amsterdam
45. Ramakrishnan N, Arunachalam VS (1993) J Am Ceram Soc 76:2745
46. Martin LP, Dadon D, Rosen M (1996) J Am Ceram Soc 79:1281
47. Rice RW (1996) In: Liu D-M (ed) Porous ceramic materials: fabrication, characterisation, applications. Trans Tech Publications, Zurich, p 1
48. Rice RW (1996) J Mater Sci 31:102
49. Roberts AP, Garboczi EJ (2000) J Am Ceram Soc 83:3041
50. Budiansky B (1965) J Mech Phys Solids 13:223
51. Wu TT (1966) Int J Solids Struct 2:1
52. Mori T, Tanaka K (1973) Acta Metall 21:571
53. Dvorak GJ, Srinivas MV (1999) J Mech Phys Solids 47:899, 2207
54. Dunn ML, Ledbetter H (1995) J Mater Res 10:2715
55. Luo J, Stevens R (1996) J Appl Phys 79:9047
56. Ferrari M, Filipponi M (1991) J Am Ceram Soc 74:229
57. Ponte Castañeda P, Willis JR (1995) J Mech Phys Solids 43:1919
58. Rice RW (1996) J Mater Sci 31:1509
59. Cytermann R (1987) Powder Metall Int 19:27
60. Phani KK, Niyogi SK (1987) J Am Ceram Soc 70:362
61. Boccaccini AR, Ondracek G, Mazilu P, Windelberg D (1993) J Mech Behav Mater 4:119
62. Arnold M, Boccaccini AR, Ondracek G (1996) J Mater Sci 31:1643
63. Abdel-Ghani M, Petrie JG, Seville JPK, Clift R, Adams MJ (1991) Powder Technol 65:113
64. Skriver HL, Rosengaard NM (1992) Phys Rev B 46:7157
65. Hentschel ML (2002) PhD thesis. The University of Newcastle
66. German RM (1996) Sintering theory and practice. Wiley, New York
67. Rice RW (2005) J Mater Sci 40:983